

Northumbria Research Link

Citation: Ganjehlou, Hamed Ganjeh, Niaei, Hadi, Jafari, Amirreza, Aroko, Daniel, Marzband, Mousa and Fernando, Terrence (2020) A Novel Techno-Economic Multi-Level Optimization in Home-Microgrids with Coalition Formation Capability. Sustainable Cities and Society, 60. p. 102241. ISSN 2210-6707

Published by: Elsevier

URL: <https://doi.org/10.1016/j.scs.2020.102241>
<<https://doi.org/10.1016/j.scs.2020.102241>>

This version was downloaded from Northumbria Research Link:
<http://nrl.northumbria.ac.uk/id/eprint/43217/>

Northumbria University has developed Northumbria Research Link (NRL) to enable users to access the University's research output. Copyright © and moral rights for items on NRL are retained by the individual author(s) and/or other copyright owners. Single copies of full items can be reproduced, displayed or performed, and given to third parties in any format or medium for personal research or study, educational, or not-for-profit purposes without prior permission or charge, provided the authors, title and full bibliographic details are given, as well as a hyperlink and/or URL to the original metadata page. The content must not be changed in any way. Full items must not be sold commercially in any format or medium without formal permission of the copyright holder. The full policy is available online: <http://nrl.northumbria.ac.uk/policies.html>

This document may differ from the final, published version of the research and has been made available online in accordance with publisher policies. To read and/or cite from the published version of the research, please visit the publisher's website (a subscription may be required.)

A Novel Techno-Economic Multi-Level Optimization in Home-Microgrids with Coalition Formation Capability

Abstract

In recent years, microgrids (MG's) have operated in the power systems for various reasons such as reduction of energy losses, improvement of voltage stability and grid reliability. The implementation of Home Microgrid (H-MG) has proven successful in tackling these issues. This paper proposes a novel techno-economic multi-level optimization method and modern time varying price model aimed at encouraging participation in a coalition system, minimizing energy cost of a Home Microgrid (H-MG) and investigate the impact it has on voltage stability and reliability of the grid. The intended H-MG includes an apartment with several units which consist of electrical and thermal energy generators, energy storage devices and can trade energy within the H-MG's and the upstream network. The proposed method develops an algorithm for smart charging/discharging of energy storage and electric vehicles (EV) to improve energy efficiency. The performance of the proposed algorithm is tested on several electrical and thermal loads configurations, the IEEE 15 and 33-bus networks are used to prove the efficiency of the coalition system between the H-MG on a large scale. The simulations are implemented on MATLAB software and results indicate an improvement in voltage profiles and grid reliability.

Keywords: Transactive energy; coalition formation; reliability; voltage stability; integrated homemade microgrid.

Nomenclature

Index and sets

n	Index of number of bus
n'	Index of load
s	Index of unit number
t	Index of hours
e	Electrical Power
h	Heat or Thermal Energy

Parameters and Constants

k_1, c_1	Parameters of Weibull distribution function
μ	The average value of data
σ^2	The variance value of data
A_e	The cross-sectional area of photovoltaics [m^2]
η	The efficiency of photovoltaics [%]
$\underline{ES}_e / \overline{ES}$	The minimum/ maximum allowable state of charge of battery [kWh]
$\underline{P}_e^{ES} / \overline{P}_e^{ES}$	The minimum/ maximum allowable power of battery [kW]
\overline{P}^{DW}	The nominal power of dishwasher [kW]
\overline{P}^{REF}	The nominal power of refrigerator [kW]
$\underline{E}^{EV} / \overline{E}^{EV}$	The minimum/ maximum allowable state of charge of EV [kWh]
E_t^{EV}	The charging value of the EV [kWh]
$\underline{P}^{EV} / \overline{P}^{EV}$	The minimum/ maximum allowable power of battery [kW]
$\underline{P}_{s,g}^{CHP} / \overline{P}_{s,g}^{CHP}$	The minimum/ maximum generated electrical power of CHP [kW]
$\eta_e^{CHP} / \eta_h^{CHP}$	The electrical/ thermal efficiency of CHP [%]
$P_{t,h}^{HHW}$	The nominal thermal power of water heater [kW]
$\eta_{t,h}^{HHW}$	The thermal efficiency of water heater [%]
$\overline{P}_{t,g}^{GB}$	The maximum generated electrical power of gas boilers [kW]

$\eta_{t,h}^{GB}$	The thermal efficiency of gas boilers [%]
$\overline{P}_{e,s}^{CHP}$	The electrical maximum capacity of CHP [kW]
MCP_t	The market price of electricity [£/kW]
GFC	The gas fuel cost [£/kW]
MIN_{price}	The minimum price of power exchange [£/kW]
N_{bus}	Number of busses

Functions and Variables

I_t^β	The solar irradiation intensity [kW/m ²]
P_t^{PV}	The output power of photovoltaics [kW]
$P_{t,e}^{ES}$	The charging and discharging power of battery [kW]
$E_{t,e}^{ES}$	The charging value of the battery [kWh]
X_t^{DW}	The binary variable for on-off state of dishwasher
$P_{t,e}^{DW}$	The power consumption of dishwasher [kW]
X_t^{REF}	The binary variable for on-off state of refrigerator
$P_{t,e}^{REF}$	The power consumption of refrigerator [kW]
P_t^{EV}	The charging and discharging power of EV [kW]
$P_{t,g}^{CHP}$	The generated electrical power of CHP from natural gas [kW]
$P_{t,e}^{CHP} / P_{t,h}^{CHP}$	The generated electrical/ thermal power of CHP [kW]
X_t^{HHW}	The binary variable for on-off state of water heater
$P_{t,g}^{GB}$	The generated electrical power of gas boilers from natural gas [kW]
$P_{t,h}^{GB}$	The generated thermal power of gas boilers [kW]
$P_{s,t}^{PV}$	The generated power of PV [kW]
$P_{s,t}^{WT}$	The generated power of WT [kW]
$P_{s,t}^{AEL}$	The power consumption of AEL [kW]
$P_{emp,s,t}^{CHP}$	The empty capacity of CHP [kW]
$P_{s,t}^{CHP}$	The generated electrical power of CHP to supply own unit [kW]
$P_{s,t,h}^{CHP}$	The generated thermal power of CHP to supply own unit [kW]
$P_{s,t}^{TSP}$	The generated thermal power of TSP to supply own unit [kW]
$P_{s,t,h}^{HHW}$	The power consumption of water heater [kW]
$P_{s,t}^{ATL}$	The power consumption ATL [kW]

$P_{s,t}^{\text{grid}}$	The purchased power from main grid [kW]
P_{grid}	Part of the load power supplied by the network [kW]
P_{local}	Part of locally supplied load power [kW]
P_{Load}	The power of the load [kW]
$\text{Income}_{s,t}^{+\text{CHP}}$	The income of selling excess capacity of CHP's [£]
$\text{Income}_{s,t}^{+\text{storage}}$	The income of selling excess capacity of energy storage [£]
$\text{Income}_{s,t}^{+\text{RES}}$	The income of selling excess capacity of renewable sources [£]
I_{Load}	The current of the load [A]
I_{local}	Part of locally supplied load current [A]
I_{grid}	Part of the load current supplied by the network [A]
V_n	The voltage value [kV]
$E_{n,s,t}$	The amount of demanded energy for each load [kWh]
$E'_{n,s,t}$	The received energy of each load [kWh]

1. Introduction

Researchers have proven implementation of H-MG in the reduction of electricity cost and improvement of grid reliability. The application of H-MG enables consumers to regulate their energy consumption and trade excess energy generated in order to reduce energy cost. Coalition system is a group of H-MG's cooperating in order to meet energy demands of consumers and avoid the cost of buying energy from the upstream network.

Building energy management is considered a subset of energy management of networks. This issue is one of the most attended subjects in the field of energy management. Recently, several published papers have focused on this issue. In [1, 2], hourly scheduling and day-ahead optimization method has been proposed for energy management in the smart building to reduce the cost of the energy and improving user comfort. Home energy management in grid connected building

14 using hardware resources and software applications suggested in [3] to minimize
15 operational cost of the building and improve resiliency of the system. In [4], an al-
16 gorithm has been proposed to the optimization of MG operation based on the vari-
17 ation of ant colony algorithm in terms of reliability, scheduling of generators and
18 unit commitment for a day ahead period. In [5], a comprehensive framework for
19 optimal energy management in smart commercial buildings has been investigated.
20 The main objectives are cost minimization and maximization of the comfort level
21 of customers using several small-scale load. In [6], optimal capacity and type of re-
22 newable energy resources (RES) have been determined by considering the planning
23 and scheduling of generation resources.

24 Moreover, optimal scheduling of a H-MG consisting of renewable and conven-
25 tional power generations with integrated responsive load and storage have been
26 discussed in [7, 8]. In [9], a comprehensive optimization approach considering
27 positive penetration of renewable energy source accompanied by demand response
28 program (DRP) has been performed to increase the profit and mitigate the cost in
29 the MG's. A hierarchical energy management system (EMS) for multiple home en-
30 ergy with the aim of maximizing financial profit and peak shaving of the network
31 demand has been studied in [10]. Dynamic planning for energy management in
32 smart homes with plug-in electric vehicles (EV) to the minimization of cost and
33 dissatisfied consumers has been presented in [11]. In [12] it is proven that by a
34 systematic procedure, occupants of the building can reduce their energy consump-
35 tion by up to 20% via improving their behavior based on direct feedback of the
36 system.

37 In [13], a system for energy management in H-MG's has been experimentally de-
38 signed. In addition, the multi-period artificial bee colony algorithm has been used
39 to minimize the operational cost of the H-MG system. [14] provides an energy
40 management system for smart homes with novel multi-restricted scheduling under
41 the time of use pricing by grey wolf optimizer. In [15], an investigation of the en-
42 ergy interaction of interconnected MG's have been performed using two distributed
43 interaction algorithms and price signals.

44 The interconnection of H-MG's for competing in the market and maximizing

profit has been suggested in [16]. In this paper, the economic power dispatch is performed by using the artificial bee colony algorithm. In [17], the main topic is “energy management in the retail market”. Hence, the noted study discusses participation of actors in the energy market along with the interaction of the MG components with other MG’s and the network. In [18], the profit maximization of distributed energy resources (DER) through “coalition formation” has been presented. Plus, various participants have been encouraged to participate in coalition formation by presenting a smart pricing mechanism due to the high range of production and shortage in power. Reference [19] has investigated the collaboration of H-MG with distributed active systems and the retail electricity market. This paper investigates the implications of the distributed active systems including DRP, various resources and storage. In [20], a new framework has been suggested for smart transactive energy of H-MG with coalition formation. Also, thermal and electrical resources have been optimally utilized, accordingly. This study encourages players to participate in the market by ensuring profits will be made. Reference [21] performs the optimal management of thermal/electrical energy resources in the presence of energy storage system (ESS) on the residential scale. In addition, the cost of the system has been reduced by combining DRP, plug-in EV’s and thermal energy storage (TES). A new method for optimal allocation and energy management of ESSs has been presented in [22], to reduce the total energy loss of the network.

Generally, H-MG is a subset of the distribution network and power system, while the main objective of the power system is to satisfy all customers. Placing the voltage within the permissible range and providing electricity in all buses are the most significant factors that satisfy the customers. In [23], different aspects of utilizing RES, in a MG, such as environmental issues, economic factors, and reliability have been discussed. A strategy has been presented to improve network reliability and energy cost by DRP and battery technology in an isolated microgrid [24]. In other works, the minimization of capital, maintenance, operation, and replacement costs, as well as reliability enhancement have been investigated in an off-grid house [25]. The coordination of energy management and voltage control has been presented in an "islanded MG" through handling active power exchanged between MG’s and

76 EV's in [26].

77 In order to improve the reliability and the voltage, a dynamic partitioning model
78 has been presented in [27], which minimizes the not supplied active and reactive
79 power and improves the voltage deviation index. In addition, [28] has proposed
80 a hybrid algorithm for dynamic and multi-objective reconfiguration of the network
81 to improve reliability and total cost of the network. Among the reviewed literature,
82 the following shortcomings were identified:

- 83 • Consideration of apartment buildings which are the most common type of
84 building's in urban areas.
- 85 • Electrical and thermal interconnections between H-MG's and its effect on volt-
86 age stability and grid reliability
- 87 • The effect of Electric Storage (ES) and Thermal Energy Storage (TES) on the
88 efficiency and cost of operating a H-MG.
- 89 • A comparison between the coalition of H-MG and non-coalition of H-MG.
- 90 • A consideration of the economic and technical constraints of operating H-
91 MG's in a coalition system.

92 Different heuristic optimizers, like GAMS, solve optimization problems and ob-
93 jectives as a single problem. The utilization of these methods in solving optimization
94 problems with a high number of technical constraints have several complications
95 due to increasing problem non-linearity. In this regard, this paper solves the H-MG
96 management problem by a novel techno-economic approach, as a multi-level opti-
97 mization. The proposed method solves the described problem with several techni-
98 cal constraints and simultaneously optimizes the economic objectives. While other
99 methods cannot effectively solve these types of problems, and only minimizes the
100 economic objectives and not capable of considering the technical constraints holis-
101 tically. By linearizing and prioritizing the problem, the proposed optimizer enables
102 the consideration of nonlinear technical constraints and solves the problem in the
103 shortest time without any iteration.

104 The main contributions of this paper are as follows:

- 105 • Presenting a novel techno-economic multi-level optimization method for en-
106 ergy management of H-MG's.

- 107 • Introducing a new method for charging/discharging of the storage and EV's
108 to enhance their performance.
- 109 • Effective policy-making and pricing strategy to encourage consumers to par-
110 ticipate in the coalition system.
- 111 • Presenting a new electricity pricing approach by using elasticity and before-
112 day market information.
- 113 • New policymaking to reduce the cost and dependence of players on the net-
114 work and increase their reliability.
- 115 • Proposing efficient policies for power exchange of CHP's, thermal storage's
116 and GB's between H-MG's.

117 The remainder of the paper is as follows. Section 2 introduces the model of
118 different components and concepts of the problem. In section 3, the problem for-
119 mulation of paper is presented, Section 4 develops a novel methodology for the
120 desired H-MG. Finally, Section 5 and 6 demonstrate numerical results and conclu-
121 sions of the paper, respectively.

122 2. Modeling

123 The general structure of the H-MG's and the modeling of the RES's power gener-
124 ation are introduced in [Section 2.1](#). Components modeling not represented in this
125 paper, and contents are similar to [20].

126 2.1. The H-MG structure

127 As seen in Figure 1, the intended H-MG is an apartment building consisting of
128 five units with independent occupants that participate in a coalition, to reduce the
129 total cost of the H-MG. Each unit is equipped with photovoltaics (PV), wind turbine
130 (WT), combined heat and power (CHP), gas boiler (GB), solar water heater, bat-
131 tery, thermal storage tank and EV for generating and storing electrical and thermal
132 energy. The electrical loads considered for each home includes a freezer, a dish-
133 washer, an EV, and an aggregated electrical load (AEL). In addition, thermal loads
134 include hot water and an aggregated thermal load (ATL). In the considered H-MG,

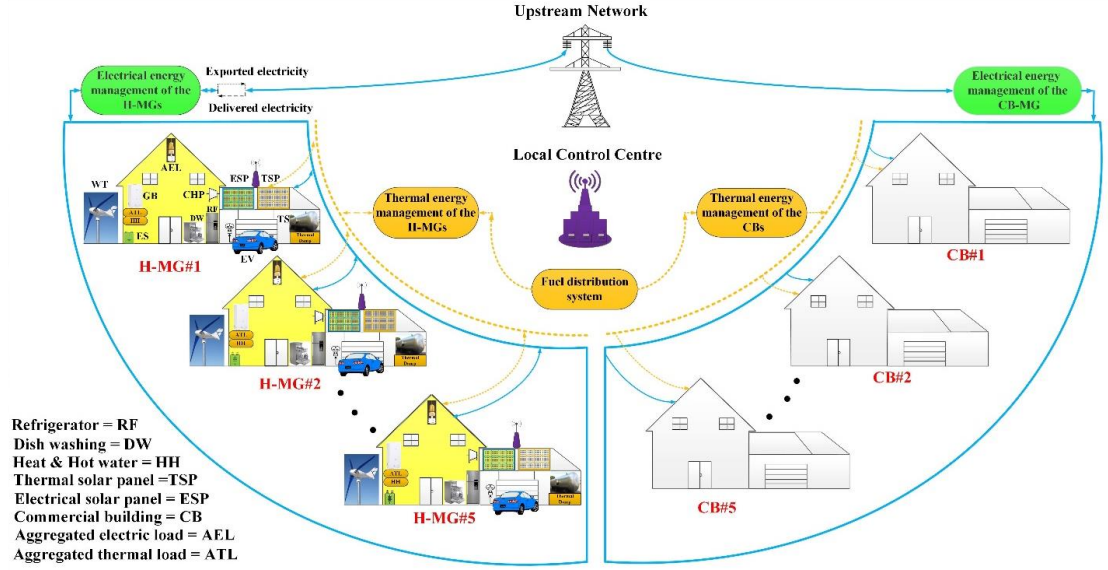


Figure 1: The schematic view of desired H-MG

all units can connect to the local electrical and thermal network. Also energy will be traded between the H-MG's. The H-MG will connect to the main grid, and power exchanges are considered with bilateral contraction.

2.2. The Modeling of Renewable Power Generation

Due to various environmental factors, RES, such as PVs and WTs, have probabilistic output. In this regard, the normal and Weibull probabilistic functions are used for modeling the output power of PV's and WT's, respectively. The hourly data for wind speed and solar irradiation corresponding to London city have been collected for one month [29?]. Also, solar irradiation and wind speed have been randomly generated for one day, based on the average and variance value of desired data. The Weibull and normal distribution functions are shown in Eqs. (1) and (2), respectively [24].

$$f(v) = \frac{k_1}{c_1} \left(\frac{v}{c_1} \right)^{k_1-1} \exp\left(-\left(\frac{v}{c_1}\right)^{k_1}\right) \quad (1)$$

$$h(v, \mu, \sigma^2) = \frac{1}{\sqrt{2\pi\sigma^2}} \exp\left(-\frac{(v - \mu)^2}{2\sigma^2}\right) \quad v \in \mathbb{R} \quad (2)$$

where, k_1 and c_1 are Weibull parameters, and μ and σ_2 are the average and variance of data, respectively. To generate random data for wind speed, first k_1 and c_1 coefficients are obtained, then wind speed is calculated for one day [30].

3. Problem Formulation

The formulation of different components of the desired H-MG is introduced in this section.

3.1. The Output Power of PV's and Solar Water Heater

Power generation of PV's and solar water heaters [31] depends on their technical specifications and the amount of solar irradiation, which is calculated as Eq. (3) [20]. In this study, the thermal energy loss in the water heater is ignored.

$$P_t^{PV} = A_c \eta I_t^\beta \quad (3)$$

3.2. The Power Distribution between Batteries and EV's

In this paper, the charging and discharging of batteries and EV's are executed proportionally to the State of Charge (SOC) of the energy storage's. The reason behind charging EV's and ES's in proportion to its SOC is to allow, even distribution of excess energy available in the network instead of excess energy from a H-MG utilized only by the EV and batteries of the home. Also, it's possible, the storage (which has energy) may not be unable to assist other H-MG's more than its nominal power. Therefore, the excess energy is distributed uniformly between all batteries and EV's. This strategy can be applied to the systems with the coalition. For excess power (P), the charging power of batteries are as follows:

$$P_{s,t,e}^{ES} = P \times \frac{\bar{P}_{s,e}^{ES}}{\sum_{s=1}^m \bar{P}_{s,e}^{ES}} \quad (4)$$

3.3. CHP

The proposed model for CHP and its constraints are as following equations [20]:

$$P_{s,t,e}^{CHP} \leq P_{s,t,g}^{CHP} \leq \bar{P}_{s,g}^{CHP} \quad (5)$$

$$P_{s,t,e}^{CHP} = \eta_e^{CHP} \times P_{s,t,g}^{CHP} \quad (6)$$

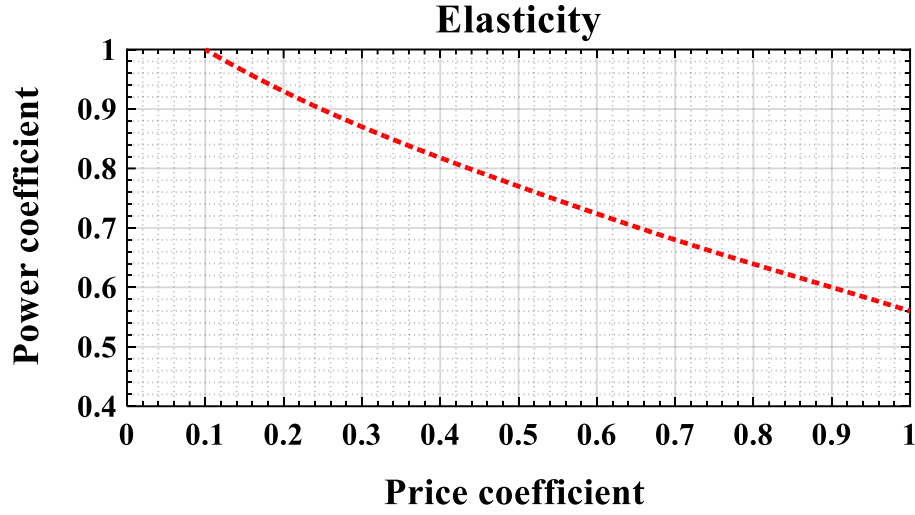


Figure 2: The price elasticity curve

175

$$p_{s,t,h}^{CHP} = \eta_h^{CHP} \times p_{s,t,g}^{CHP} \quad (7)$$

176 According to Eq. (5), the generated power by CHP's would remain within the
 177 upper and lower limit of its capacity. In addition, Eqs. (6) and (7) shows the elec-
 178 trical and thermal efficiency co-efficient of CHP's. Modeling of other equipment in
 179 the MG's structure is similar to equipment and resource modeling in [20].

180 3.4. Power Exchanged with the Main Grid

181 Figure 2 illustrates the curve of power coefficient in terms of price coefficient,
 182 known as the "price elasticity curve". According to Figure 2, the H-MG must offer a
 183 price lower than the main grid's Market Clearing Price (MCP) in order to facilitate
 184 the sale of excess power to the grid and vice versa, by increasing the salable power.
 185 The profit of selling electricity to the main grid is obtained by Eq. (8).

$$\text{Profit}^+ = (\text{power coefficient} \times \text{salable power}) \times (\text{price coefficient} \times \text{MCP}) \quad (8)$$

187 3.5. The Objective Function in the Coalition System

188 The cost, income and overall objective function of the system are introduced as
 189 the following equations, respectively.

$$\begin{aligned}
190 \quad \text{Cost} &= \sum_{t=1}^{24} \sum_{s=1}^5 \left[P_{s,t}^{\text{grid}} \times \text{MCP}_t + (P_{s,t,g}^{\text{CHP}} + P_{s,t,g}^{\text{GB}}) \times \text{GFC} + \text{EX}_{e,s,t}^{-\text{coalition}} \times \text{MIN}_{\text{price}} \right. \\
191 \quad &\quad \left. + \text{EX}_{e,s,t}^{-\text{CHP}} \times \text{MCP}_t + \text{EX}_{h,s,t}^{-\text{coalition}} \times 3 \times \text{GFC} + \text{EX}_{h,s,t}^{-\text{GB}} \times 1.1 \times \frac{\text{GFC}}{0.85} \right] \quad (9) \\
192 \quad \text{Income} &= \sum_{t=1}^{24} \sum_{s=1}^5 \left[\text{profit}_{s,t}^{+\text{CHP}} + \text{profit}_{s,t}^{+\text{RES}} + \text{profit}_{s,t}^{+\text{storage}} + \text{EX}_{e,s,t}^{+\text{coalition}} \times \text{MIN}_{\text{price}} \right. \\
&\quad \left. + \text{EX}_{e,s,t}^{+\text{CHP}} \times \text{MCP}_t + \text{EX}_{h,s,t}^{-\text{coalition}} \times 3 \times \text{GFC} + \text{EX}_{h,s,t}^{-\text{GB}} \times 1.1 \times \frac{\text{GFC}}{0.85} \right] \quad (10) \\
&\quad \text{Total cost} = \text{Cost} - \text{Income} \quad (11)
\end{aligned}$$

193 where GFC is the Gas Fuel Cost and $\text{EX}_{e,s,t}^{-\text{coalition}}$ is the received power of the s^{th} home
 194 from other H-MG's at hour t prior to operating own CHP's. If a unit wants to supply
 195 the required electricity from own CHP, it has to spend as much as $\text{GFC}/0.34$ that is
 196 more than offered value by other H-MG ($\text{MIN}_{\text{price}} = \text{£}0.03$). In addition, if all H-MG
 197 have maximised storage capacity, the excess is sold to the network. The lowest price
 198 is 0.1 of the market's lowest price that is lower than 0.03£, so the coalition policy is
 199 reliable in terms of cost and reliability. Also, $\text{EX}_{e,s,t}^{-\text{CHP}}$ is the received power of the
 200 s^{th} home from neighbors at hour t after operating own CHP's. If the owner cannot
 201 supply their required power needs from their own CHP's, it has to be supplied from
 202 EV's or CHP's of other units or storage's. If the EV's and storage's are considered
 203 as the first priority, it would not be economical to buy energy from other H-Mg's at
 204 peak period. Also, during the CHP's operation, utilization of boilers is decreased,
 205 and operation performance is improved by supplying power from other units CHP's.
 206 Therefore, the owner can supply power shortage from neighbors at 0.9 of the market
 207 price and keep EV's and storage for emergencies.

208 In Eqs. (9) and (10), $\text{EX}_{e,s,t}^{-\text{GB}}$ is the received thermal power of the s^{th} home from
 209 neighbors at hour t after operating own boilers. If a unit experiences shortage of
 210 thermal energy, it has to buy it from other unit's boilers or thermal storage. Since
 211 there is no common market for buying and selling thermal energy, this energy is
 212 exchanged between the adjacent H-MG's to supply the thermal load of the H-MG.
 213 Thermal storage's are used as a backup, so the owner has to supply shortage from
 214 adjacent storage's at three times the gas price, but still prefers to buy from adjacent
 215 boilers at the price of $1.1 \times \text{GFC}/0.85$.

216 3.6. The Objective Function of Non- Coalition System

217 In non- coalition system, due to lack of power exchange between H-MG, the total
218 objective function is modeled as Eq. (12). In this equation, the first and second term
219 is related to the total cost and the total income of the system.

$$\text{Total cost} = \left[\sum_{t=1}^{24} \sum_{s=1}^5 p_{s,t}^{\text{grid}} \times \text{MCP}_t + (P_{s,t,g}^{\text{CHP}} + P_{s,t,g}^{\text{GB}}) \times \text{GFC} \right] - \left[\sum_{t=1}^{24} \sum_{s=1}^5 \text{profit}_{s,t}^{\text{CHP}} + \text{profit}_{s,t}^{\text{RES}} + \text{profit}_{s,t}^{\text{storage}} \right] \quad (12)$$

221 3.7. The Impact of the H-MG on the Main Grid Reliability

222 H-MG improves voltage quality and increases the reliability of the distribution
223 system. This section introduces the different effects of a H-MG on the main grid.
224 The current value in each bus is obtained from the following relation:

$$|I_{\text{Load}}| = |I_{\text{local}} + I_{\text{grid}}| = \frac{|P_{\text{local}} + I_{\text{grid}}|}{|V|} = \frac{|P_{\text{local}}|}{|V|} \quad (13)$$

226 If the value of P_{local} is increased, P_{grid} is simultaneously decreased. So, the line's
227 current and losses are reduced and the voltage profile is improved. Thereby, the
228 dependency on the main grid is decreased and reliability is enhanced.

229 A: The Voltage Quality of the Main Grid

230 In this study, in order to assess the voltage quality of the main grid, the voltage
231 deviation index is calculated as Eq. (14).

$$\delta V = \sum_{n=1}^{N_{\text{bus}}} (1 - V_n) \quad (14)$$

233 In large-scale cases, three types of load are considered. The first type is buildings
234 with five units that can exchange power, the second type is not able to exchange
235 power, and the third group supplies own power from the main grid.

236 B: Reliability

237 The reliability is a significant factor in power quality assessment. One of the
238 main reliability indices is Energy Not Supplied (ENS) in Eq. (15) that is used for
239 analyzing the effect of H-MG's on the reliability of the grid network during short
240 circuit faults:

$$\text{ENS} = \sum_{t=1}^{24} \sum_{s=1}^5 \sum_{n=1}^{N_{\text{bus}}} (E_{n,s,t} - E'_{n,s,t}) \quad (15)$$

242 4. The Proposed Methodology for a H-MG with a Coalition/ Non-Coalition Sys- 243 tem

244 This section consists of two subsections, which are described in the following
245 as:

246 4.1. Coalition system

247 If electrical and thermal sources of each unit compensate the power shortages of
248 other units, the MG is called “coalition H-MG”. The proposed algorithm is explained
249 for systems with the coalition, in the following parts.

250 A: Electrical Power Management Strategy

251 The electricity management in the desired H-MG is performed according to the
252 following steps.

253 Step 1. Electrical Load Balance

254 The power balance in each unit at any time can be calculated by Eq. (16).

$$E_{balance,s,t} = P_{s,t}^{PV} + P_{s,t}^{WT} - \chi_{s,t}^{REF} \times \bar{P}_{s,t}^{REF} - \chi_{s,t}^{DW} \times \bar{P}_{s,t}^{DW} - P_{s,t}^{AEL} \quad (16)$$

256 Step 2. EV's Charging

257 The charging power of EV at any moment is calculated by Eq. (17) with a po-
258 tential to charge up to \bar{P}_s^{EV} .

$$P_{s,t}^{EV} = \bar{E}_s^{EV} - E_{s,t}^{EV} \quad (17)$$

260 Intended EV's, have charge/discharge capability which is charged at night be-
261 tween hours of 1:00 to 6:00 and are available to consumers from 6:00-16:00. Due
262 to the free capacity of resources between hours 1:00 and 6:00, there is a maximum
263 limit to charging EV's which is maximum poer capacity of the EV, \bar{P}_s^{EV} . The power
264 and energy limitations of EV's are shown in Eqs. (18) and (19), respectively.

$$\underline{P}^{EV} \leq P_{s,t}^{EV} \leq \bar{P}^{EV} \quad (18)$$

$$\underline{E}^{EV} \leq E_{s,t}^{EV} \leq \bar{E}^{EV} \quad (19)$$

267 Step 3. The Exchange of Electrical Power between H-MG

268 When a H-MG experiences shortage of power, it compensates for this shortage by
269 buying power from other H-MG's instead of the main grid. The aim is to minimize

the total cost, as other H-MG's with excess, offer power at prices lower the main grid MCP. As the unit s_2 transmit power in the amount of $EX_{e,s,t}^{-coalition}$ to the unit s_1 , the new value of the electrical balance of unit s_1 :

$$E_{balance}(s_1, t) = E_{balance}(s_2, t) + EX_{e,s,t}^{coalition} \quad (20)$$

Step 4. The Exchange of Excess Electricity between storage's

In this stage, firstly, the capacity of batteries and the amount of excess power in the apartment building are examined. Then, the excess power in the units is divided between the storage's proportional to their capacity. In doing so, in urgent conditions, the maximum power can be supplied by batteries, which causes the batteries to be optimally used.

Step 5. Buying Power from Other H-MG Energy Storage's

In this stage, the batteries of each unit compensate for the electricity shortage of other units. In this regard, the total electricity shortages of the building are determined and the storage's discharging occur based on \bar{P}_e^{ES} , \bar{ES}_e and Eq. (4).

Step 6. Compensating Power Shortage from H-MG CHP's

In this step, each unit supplies its own electrical shortage through CHP if there is a shortage of power and this shortage is greater than the CHP nominal power, the CHP operates at nominal capacity and any pending power deficit is supplied by CHP's of other units. Otherwise, CHP operates to supply as much power as needed.

Step 7. Buying Power from CHP's of other H-MG's

It is assumed that the EV's are charged between hours 1:00 and 6:00, and are discharged between hours 16:00 and 24:00. CHP's can operate up to nominal power, while storage's and EV's have limited energy and should be used as a backup. Accordingly, each unit initially utilizes own CHP and CHP's of other units, then uses storage's and EV's. However, EV's must operate prior to storage's, since EV's availability is limited. The unused capacity of CHP's is calculated by Eq. (21).

$$P_{emp,s,t} = \bar{P}_{e,s}^{CHP} - P_{t,s}^{CHP} \quad (21)$$

Step 8. The Discharge of EV's

In this step, market prices are sorted in descending order and the highly-priced hour takes higher priority. Then, the electricity shortage of all units and the remain-

ing capacity of EV's are calculated in each hour. If EV's are discharged in each hour, the discharge scheduling of EV's is carried out based on the above priority. Therefore, at the time, the market price is highest, the utilization of electrical shortage is a highest. It is assumed that H-MG occupants allow their EV's to participate in coalition formation within 16:00 -24:00. Since owners usually do not consume all energy of EV's. Hence, there is no reason to omit this extra energy as it's utilization improves reliability and reduces cost. Assuming so, market players can use EV's power within 16:00 -24:00 during peak hours and charge EV's at off-peak times or 1:00 to 6:00.

Step 9. The Charge of the Storage's

In this step, the total extra capacity of CHP's obtained, in the fourth and fifth steps and the storage capacities are determined. The nominal charging power will be equal to the difference in batteries' power limitations and their previous operation power. Since the charging cost from CHP's is less than the grid, storage's charged from the CHP's and discharged in the shortage time (in peak hours) reduces cost. The formulation of storage's are as follows:

$$P_{s,e}^{ES} \leq P_{s,t,e}^{ES} \leq \overline{P}_{s,e}^{ES} \quad (22)$$

$$ES_{s,e} \leq E_{s,t,e}^{ES} \leq \overline{ES}_{s,e} \quad (23)$$

$$E_{s,t,e}^{ES} = E_{s,t-1,e}^{ES} + P_{s,t-1,e}^{ES} \times \Delta t \quad (24)$$

Eqs. (22) and (23) indicate that the power and energy of the electrical storage should remain within the acceptable range. Also, Eq. (24) shows the calculation of the new value of the energy of electrical storage.

During peak hours, both the system with coalition formation and the network has a problem in supplying the consumers load. Therefore, it is possible to utilize batteries and distribute this amount of energy in the coalition formation system at peak hours. Thereby, improving the reliability and stability of the system voltage. It should be noted that the priority is taken into consideration of discharging the storage at high-cost hours so that, along with improving technical issues, the cost of the system can be significantly reduced.

Step 10. The Discharge of the storage's

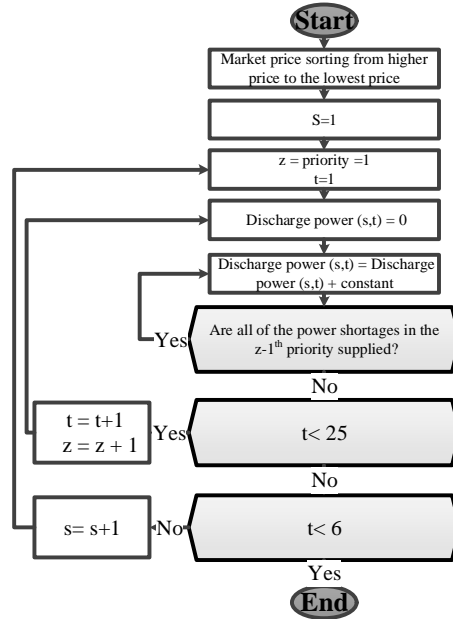


Figure 3: Discharge flowchart of the storage's

330 The market prices are sorted in descending order and the highest price has
 331 higher priority. If there is a shortage of power and batteries have energy, batteries
 332 will be discharged. The flowchart of this section is shown in Figure 3. Generally, if
 333 the algorithm is in the z^{th} priority of market price, the discharge power of storage
 334 should be increased step by step. At each step, it is checked that all power shortages
 335 in previous priority are covered. In this process, if the power shortages in previous
 336 priority are supplied properly, the incremental discharging of power continues. Oth-
 337 erwise, the powers that satisfied the condition for the last time, are determined as
 338 the discharge power of z^{th} priority.

339 Step 11. Buying Electricity from the Main Grid

340 After performing the above operations, the rest of the power shortage must be
 341 purchased from the network.

342 Step 12. Selling Excess Power to the Main Grid

343 In this step, if there is excess power in the system, it will be sold to the main
 344 grid. The excess power of RES's is offered based on the lowest price so that the grid

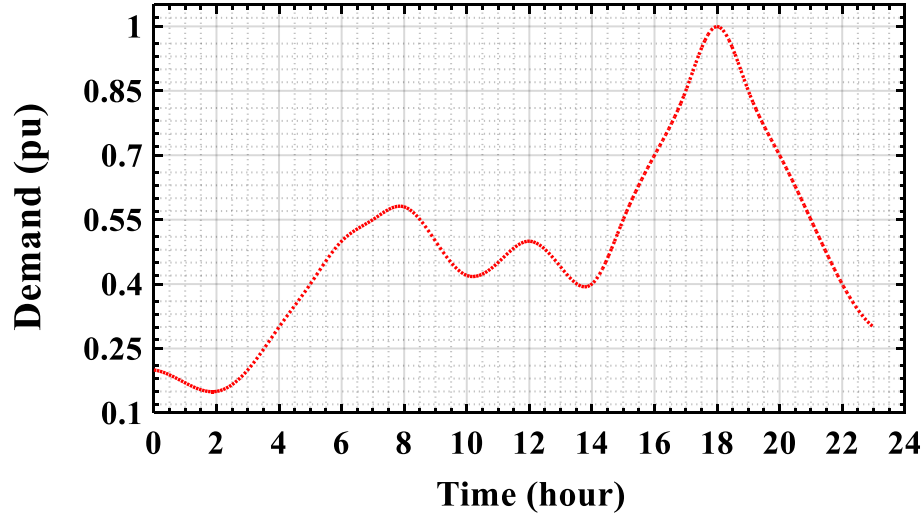


Figure 4: The general behavior of consumption in this article

345 would certainly buy it. In this condition, the system offers the main grid a lower
 346 price than the market price, considering the general demand curve of the previous
 347 day. The general behavior of consumption in the previous day is as Figure 4. This
 348 curve has been selected according to the load profile in [32, 33]. The curve is mod-
 349 ified, becomes per-unit and then its mathematical expression is obtained through
 350 the curve fitting (price coefficient). Therefore, at each moment, the offered price
 351 curve by the system is obtained by multiplying the per-unit curve by market price di-
 352 agram. The offered price and price coefficient value are determined and the power
 353 coefficient is obtained by the elasticity curve as Figure 2. The value of the power
 354 coefficient indicates the percentage of power bought by the network. It should be
 355 noted that selling excess power to the grid is not scheduled and the process can
 356 only be done in “real-time”.

357 **Step 13. Selling Excess Power Supplied by the Storage's**

358 Selling the excess electricity supplied by storage's is similar to discharging the
 359 storage's, except discharging the storage's becomes programmable while selling the
 360 excess electricity is carried out in a “real-time” manner. For mathematical modeling,
 361 firstly, it is checked that the storage's, still have energy at the end of the schedul-

ing period. If the storage's have energy, it will be discharged within hours 17:00 to 24:00, due to the high market price. At each hour, the amount of sold power by storage's based on elasticity is determined by considering this constraint in which the calculated electrical powers in steps 4, 5, 9, and 10 will remain constant. Accordingly, the amount of power that can be sold by the storage is determined as follows: the power is gradually increased from zero, and constantly is checked that there is no interruption in steps 4, 5, 9, and 10 for 24 hours. This procedure continues to up to the point that no problem occurs in performing the mentioned steps.

B: Thermal Power Management Strategy

The thermal energy management in the H-MG is performed according to the following steps.

Step 1. The Thermal Power Balance

The generation and consumption of thermal energy should be in balance according to Eq. (25).

$$T_{balance,s,t} = P_{s,t,h}^{CHP} + P_{s,t}^{TSP} - X_{s,t,h}^{HHW} \times P_{s,t,h}^{HHW} - P_{s,t}^{ATL} \quad (25)$$

Step 2. The Thermal Power Exchange between H-MG

The thermal power exchange is similar to the electricity exchange that has been explained in Step 3, part-A Section 4.1.

Step 3. The Thermal Storage Performance

In the existence of excess thermal power, it is stored in thermal storage's proportional to their capacities (Eq. (4)). If there is a unit with a thermal power shortage, it can only receive energy from own storage. In the electrical section, the main grid is considered as a backup. Also, the focus is mostly on technical issues and minimization of costs. But, in the thermal section, there is not any backup for supplying the thermal load, so other storage's are used in the last step.

Step 4. Boiler

If there is thermal energy shortage, each unit implements its boiler and supplies its load. In the case that the shortage continues, the units get help from each other. The procedure of boilers is the same as the CHP's.

Step 5. Supplying the Thermal Power Shortage from Other H-MG Thermal

392 Storage's

393 If there is further unsupplied thermal load in the system, there is no resource
394 for supplying it and the only resource is other H-MG storage's. The reason for the
395 priority of the boiler to storage's is, the maximum capacity of boilers always can
396 be used, but if the storage is used in an hour, it may not have enough energy for
397 backup at other times. Therefore, the storage of other units is used as a backup.
398 The algorithm of this section is similar to the electrical coalition section.

399 4.2. Non-Coalition System

400 This system, has no thermal and electrical exchange between units and storage.
401 All units receive power from individual generating system (RES, CHP and etc.) and
402 in the case of further excess power, the unit dumps it. Each unit stores it's excess in
403 the eventuality of a shortage, the H-MG uses it's storage. If there is a thermal power
404 shortage, the unit operates its boilers and if the boiler reaches nominal power, there
405 is no other resource for supplying shortage.

406 4.3. Concept of the Proposed Approach for Problem Optimization

407 One of the common approaches of optimization methods is considered to trans-
408 forming nonlinear problems into linear problems by conducting complex mathe-
409 matical operations. In this paper, the desired system and its behavior are studied
410 carefully, and the problem is solved as a linear problem. If the problem contains
411 n^{th} priorities, the optimal solutions will be in an n-dimensional space. It should be
412 noted that each priority is related to one of the steps of the presented method. For
413 the sake of comprehension, suppose a problem with three priorities as in Figure 5.
414 For solving the problem, first, the x-axis is evaluated and the C-point is obtained
415 (first priority). By finding point C and solving the second priority, point D is ob-
416 tained on the y-axis. Finally, by solving the third priority and specifying the third
417 point on the z axis, points E and F are obtained. As a result, each priority depends
418 on the solutions of the previous priorities.

419 The proposed method has a similarity with GAMS software considering two
420 major differences. First, in GAMS, it is very difficult to create high-level techni-

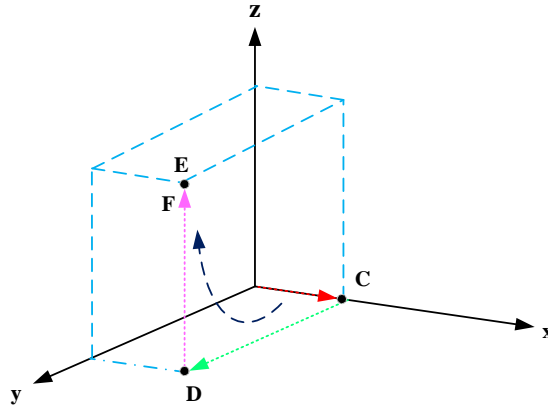


Figure 5: Schematic representation of the proposed method

cal constraints based on software codes and rules. Second, the convergence cannot be satisfied if we are facing a large number of variables along with having a nonlinear structure. Also, probing the whole solution space turns into searching n-dimensional space as the number of the variable is high and that is the difference between smart algorithms and such solvers. Also, intelligent algorithms use iterative methods to find each optimal solution, which significantly increases the running time and sometimes does not reach the absolute solution.

428 5. Results and Discussion

This study aims to investigate “H-MG’s in a coalition system” by the proposed method on small and large scales as Figure 6. In the first step, simulations are carried out for a specific load and the efficiency of the proposed method is proven. Then, the proposed method is examined based on 31 different loads, to ensure that the results are robust against load changes. Finally, the simulations are done on the IEEE 15 bus system to prove the application of the proposed coalition system in large-scale system [34]. Plus, investigations have been carried out on IEEE 33 bus system to demonstrate independence of results on the network type, [35].

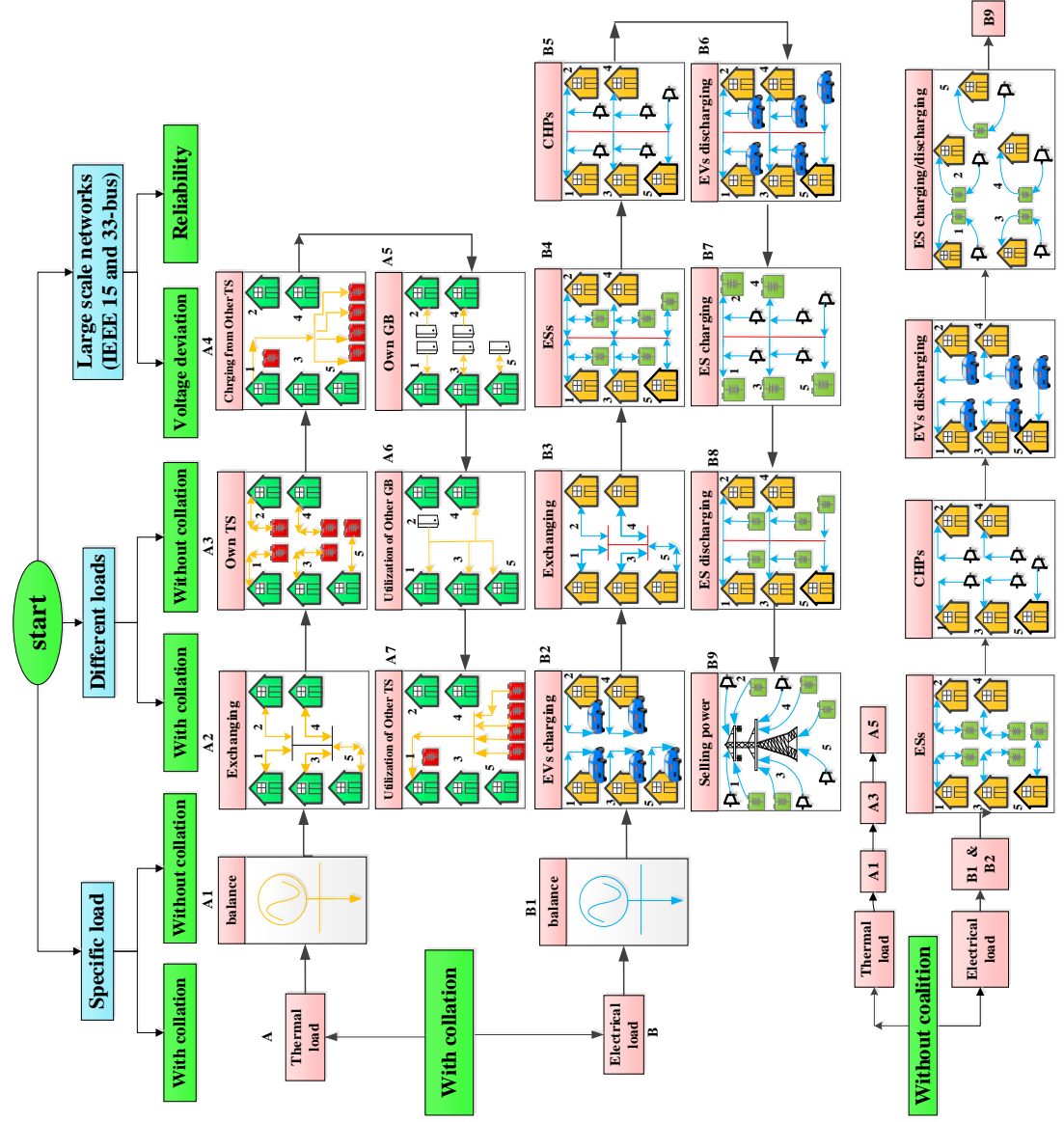


Figure 6: The general scheme of paper and the proposed sequence for H-MG management

5.1. Input Data and Scenarios

In order to analyze the effect of the coalition system on the network voltage quality, three scenarios are considered. In the first scenario, all types of loads are connected in each bus. It is assumed that twice the load of the third type is connected on each bus. In the second scenario, the first type is eliminated, and the second type is used instead to test the impact of the first type. In the third scenario, the third type of loads is replaced instead of the second type.

Table 1 shows the capacity of thermal and electrical sources. The capacity of PV's is 225W [29, 36]. The electrical and thermal efficiencies of CHP's are 34% and 40%, respectively. The efficiency of boilers is 85%, and the value of the cross-sectional area and efficiency is 1 for thermal solar panels (TSP). The charging and discharging intervals for EV's are 1:00 to 6:00 and 16:00 to 24:00, respectively. It is assumed that an EV returns to the MG at half of its capacity, and the initial energy of all storage's and EV's are set to be 0. The specifications of batteries and thermal storage's and EV's are presented in Table 2. The nominal power of the refrigerators and dishwashers are 120 W and 420 W, respectively, and their working time is every 2 hours and 1 hour in a day, respectively. It is assumed that the water heater is switched every 2 hours and its nominal power and efficiency are 1 KW and 100%, respectively. The specifications of the mentioned equipment are collected from [16, 20]. The output power of PV's and WT's are shown in Figures 7 and 8.

Table 1: Specifications of PVs, WTs, CHP's, GBs, and TSPs

Unit number	Number of PVs	WTs capacity (kW) [37]	CHP's capacity (kW)	GBs capacity (kW)	Number of TSPs
1	5	3	25	6	2
2	6	3	20	5	3
3	7	2	14	4	4
4	8	2	12	3	5
5	9	1	10	3	6

The price of gas is £0.012/KWh. The elasticity function curve and market price of electricity for all units in 24 hours are presented in Figures 9 and 10, respectively.

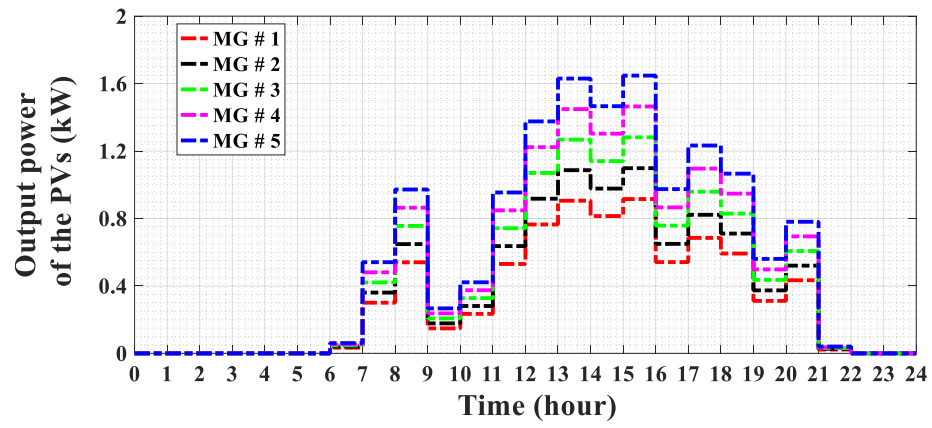


Figure 7: The output power profile of PVs.

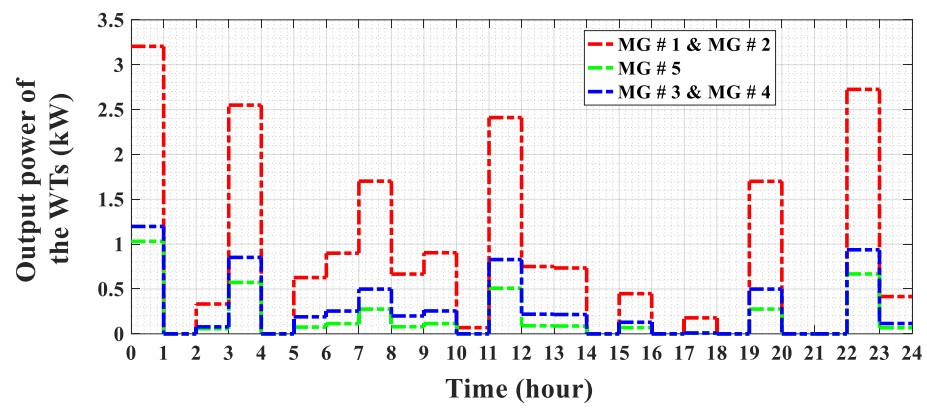


Figure 8: The output power profile of WTs.

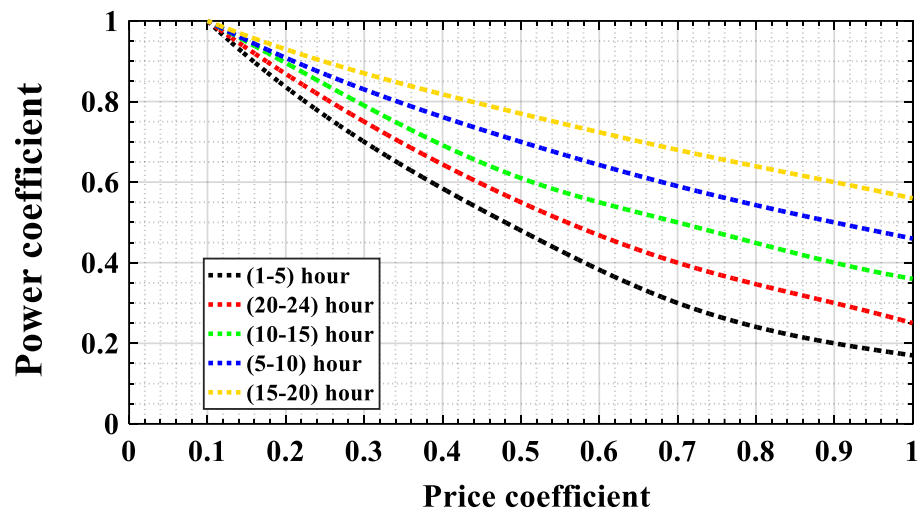


Figure 9: The price elasticity curve for different hours.

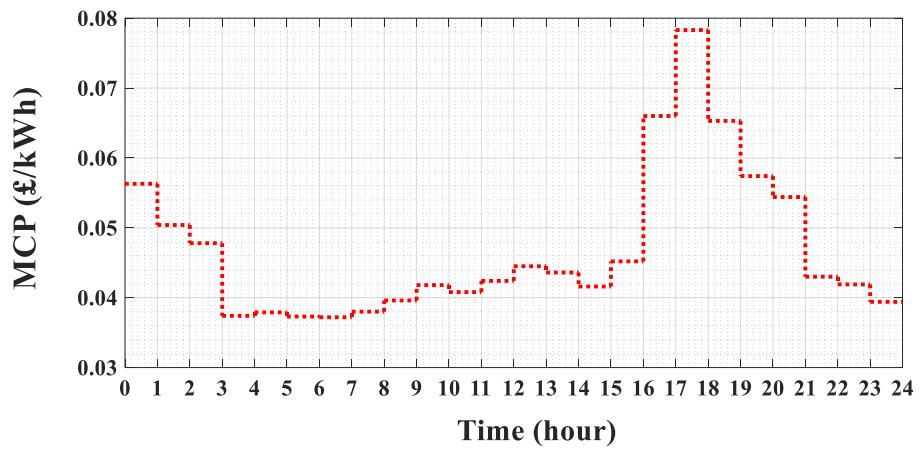


Figure 10: The market price profile.

Table 2: Specifications of thermal and electrical storage's and EV's.

Unit number	Battery power (kW)	Battery capacity (kWh)	EV power (kW)	EV capacity (kWh)	TES power (kW)	TES capacity (kWh)
1	5	20	3	9	10	20
2	5	20	3	9	10	20
3	4	16	3	9	10	20
4	4	16	3	9	10	20
5	3	12	3	9	10	20

5.2. Single H-MG with Coalition and Specific Load

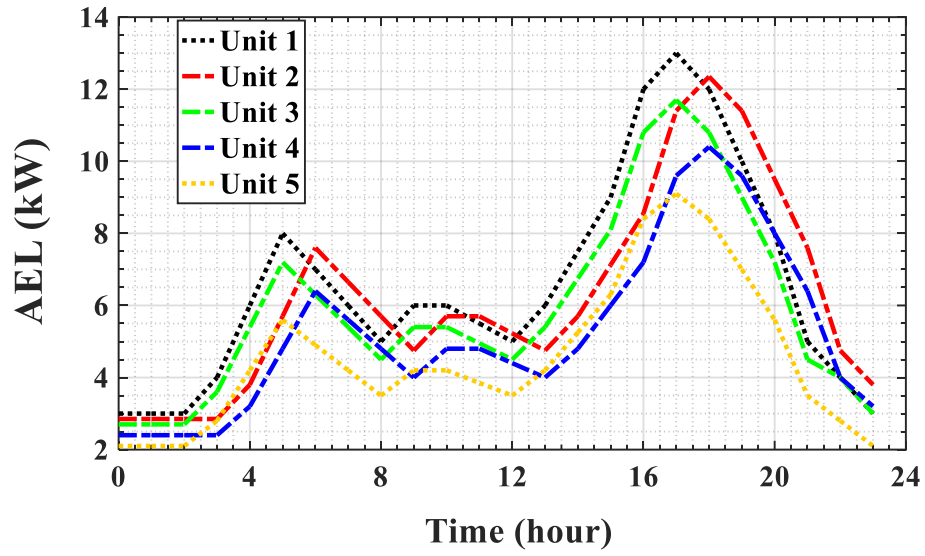
In this section, the coalition and non-coalition systems are implemented on the intended building and their results are compared. Firstly, this process is followed by a normal load, and results are obtained. The AEL and ATL are shown for 5 units in Figure 11. The different curves have been plotted for each unit with a specific color and this sequence is repeated for all figures. Each curve in the figures of this section is related to one of the units.

Figure 12 shows the electrical power shortage in the system after charging EV's that are mutual for systems with and without the coalition. Figure 12 indicates that RES's could not manage to supply different loads and EV's. In the coalition system, after charging EV's the excess power is exchanged between H-MG. However, all H-MG are faced with a power shortage at all hours, due to the lack of excess power to exchange. In addition, there is no excess power in the system; Hence, the storage's are not able to get power from the system both with and without the coalition.

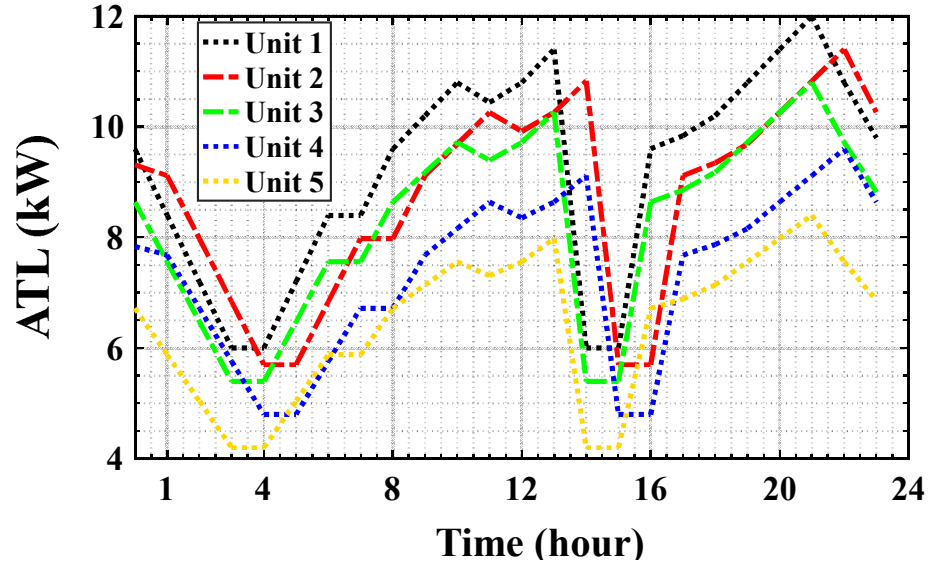
In the next step, CHP's are used to compensate for the power shortage of the system. The generated power and unused capacity of CHP's are shown in Figure 13. The electrical power shortage in the system after using CHP's are presented in Figure 14. By comparing Figures 13 and 14, it is obvious that in spite of excess capacity in CHP's, an electrical shortage is present in the system, and the H-MG's can compensate for this shortage by selling the extra power which can be generated by their CHP's.

Figure 15 shows the electrical power shortage after exchanging CHP's power between units with and without a coalition.

According to Figure 15, power shortage, cost, and reliance on the upstream network are reduced by applying the coalition system. Tables 3 and 4 show the



(a) AEL



(b) ATL

Figure 11: Curve for the first part of simulations

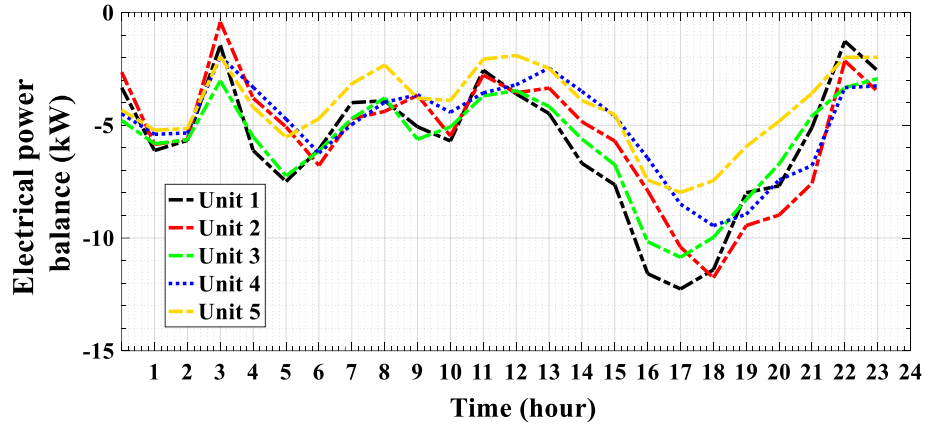
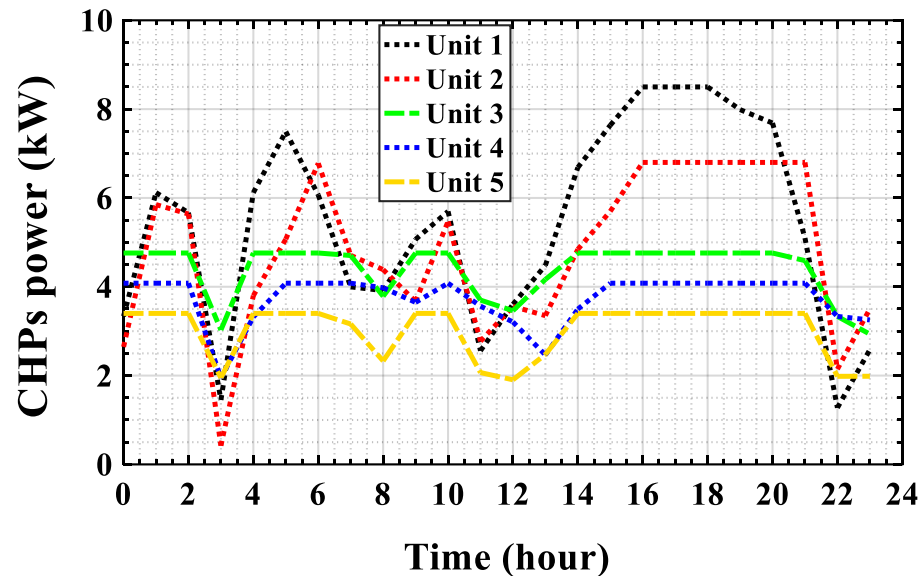


Figure 12: The electrical power shortage in the units during a day

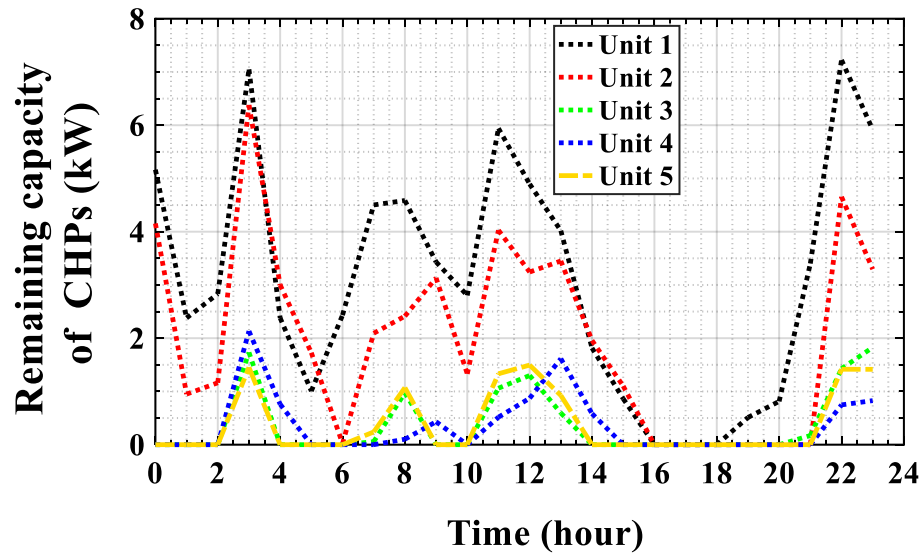
charging and discharging power of EV's for all units in the systems with and without a coalition. It is clear that during high-price hours (17:00 and 18:00), discharging energy from EV's in coalition systems is utilised more than in a non-coalition system. The total capacity of storage's is 84 kWh; if this energy can be supplied from the extra capacity of CHP, it can reduce the value of costs. The results show that prior to discharging batteries in the coalition system, the total remaining capacity of CHP's is 122.3 kWh, which storage's receive 84 kWh of the remaining CHP'S capacity. While, in non-coalition systems, the total remaining capacity of CHP's is 149. 14 kWh, which storage's only receive 67.08 kWh. According to Figure 16, storage's in the coalition system have fully charged, but, in the non-coalition system, storage's are not fully charged, and part of their charging hours have been moved to night hours. Figure 16 shows the correctness of Eq. 4 about the operation of batteries.

Total discharged energy by batteries with and without consideration of coalition is calculated as 65.6 kWh and 35.25 kWh, respectively. These results indicate that storage's are optimally managed in the coalition system. According to the high power consumption rate, the value of the sold renewable power is set to be zero. The amount of excess power of CHP's and batteries sold to the network, in both coalition modes are presented in Figures 17 and 18.

According to Figures 17 and 18, in the coalition system, most of the energy



(a) The generated power



(b) Remaining capacity

Figure 13: The generated power and the remaining capacity of CHP's

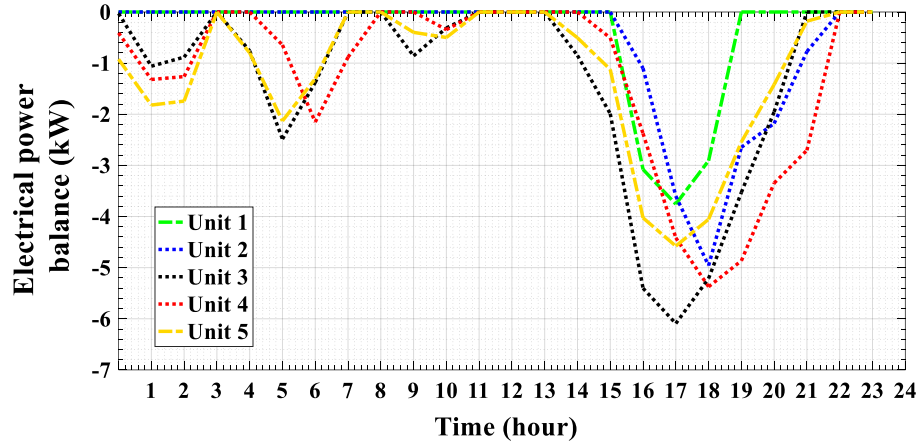
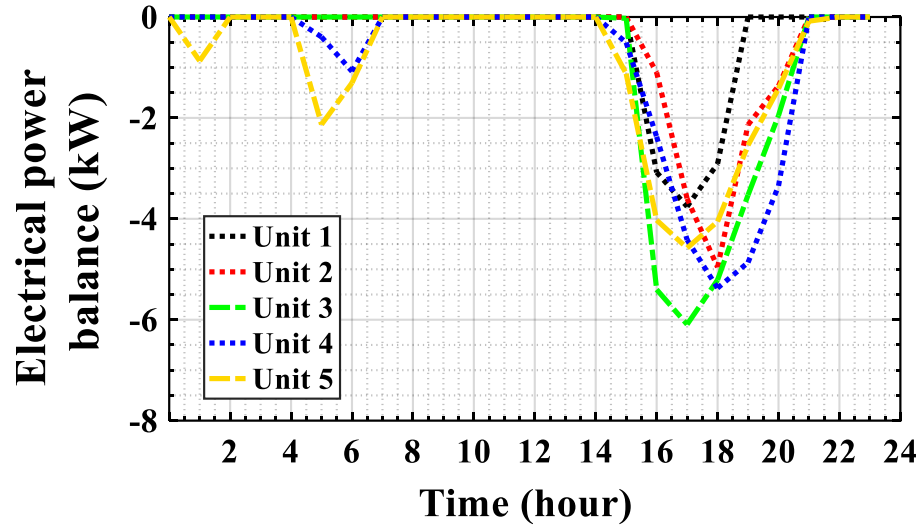


Figure 14: The amount of electrical power shortage in the system.

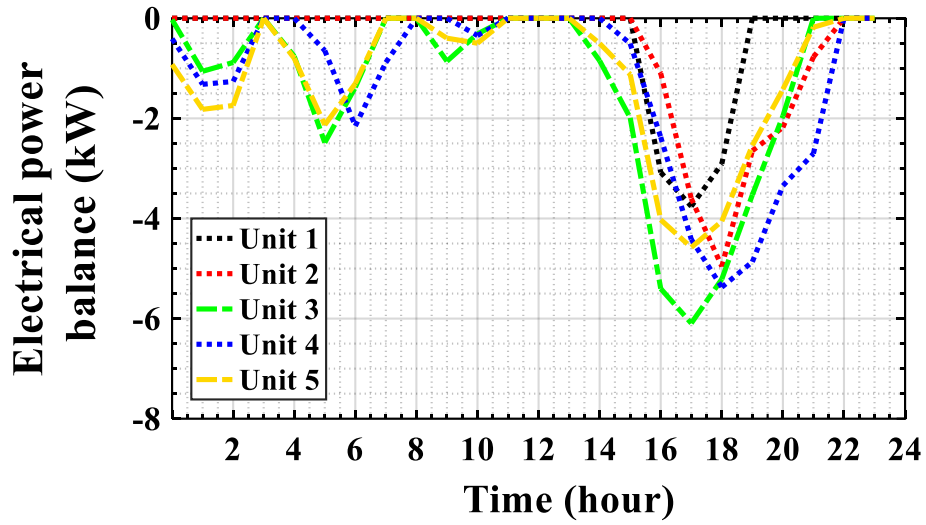
Table 3: Charging and discharging power of EV's. in the coalition system.

Unit/ hour	1 (kW)	2 (kW)	3 (kW)	4 (kW)	5 (kW)
1 to 3	3	3	3	3	3
4 to 16	0	0	0	0	0
17	-1.5	-1.5	-1.5	-1.5	-1.5
18	-3	-3	-3	-3	-3
19 to 24	0	0	0	0	0

of the resources are used in the system itself, therefore, the total energy sold in the non-coalition system has a higher value. In addition, the amount of power sold by storage's in the coalition system is in accordance with Eq. 4, that is market price and priorities. Figures 19 and 20 are related to the offered power of units to the market in the coalition and non-coalition system, respectively. Comparison of Figures 17 to 20 clearly shows that all the offered energy to market is not sold, and the tendency to sell the CHP's power at peak hours is minimum. However, this is low in coalition systems at non-peak hours. This trend is inverse for the storage's, where the additional capacity of storage's is sold at peak hours to reduce cost, and

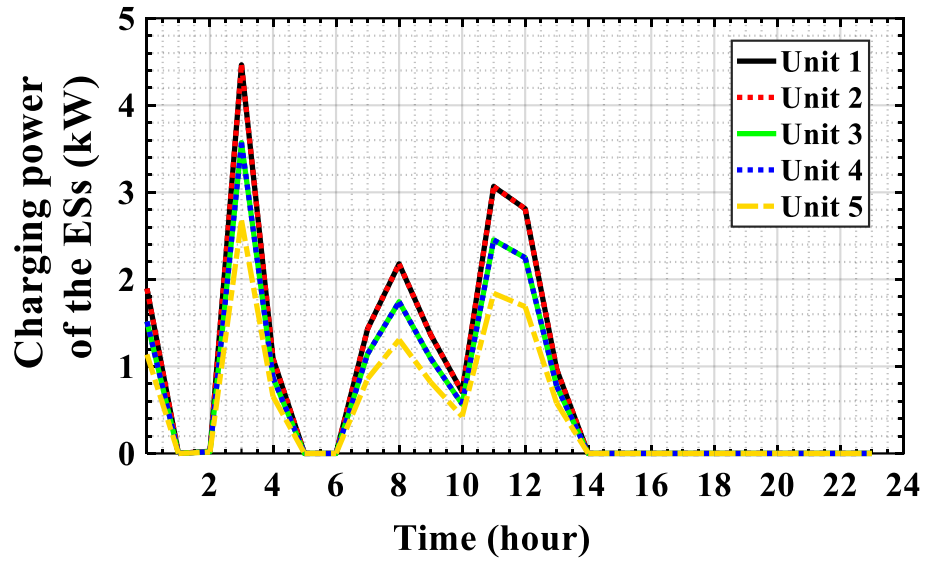


(a) With coalition

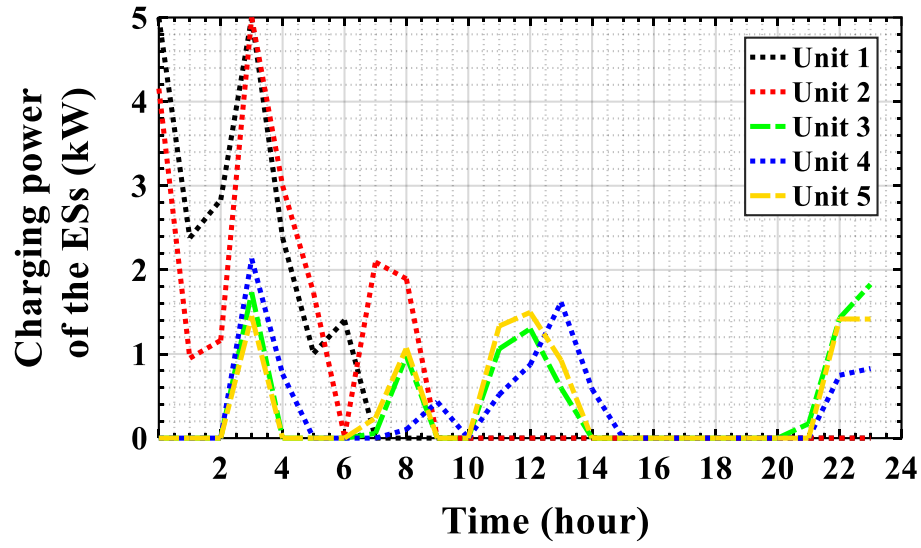


(b) Without coalition

Figure 15: The electrical power shortage in the systems

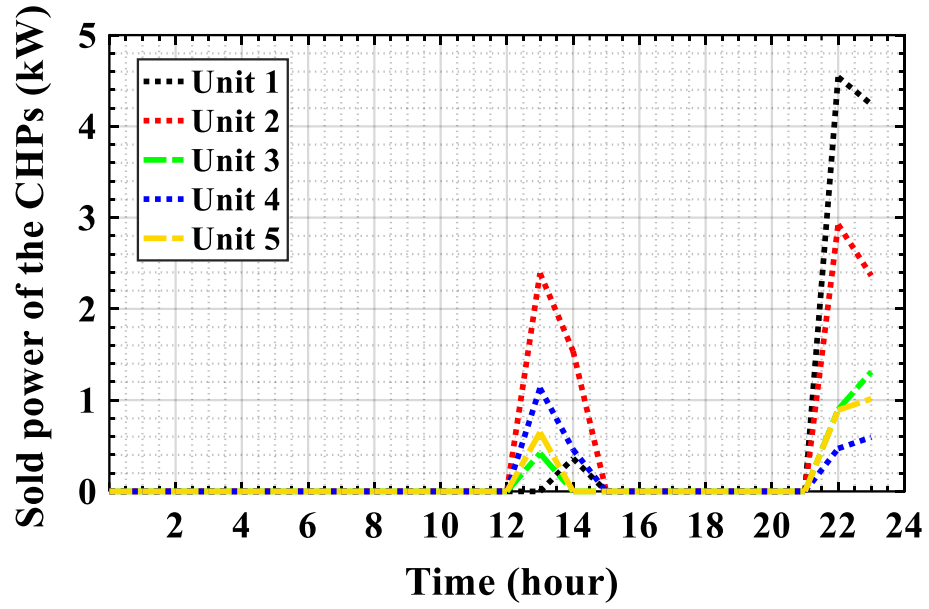


(a) With coalition

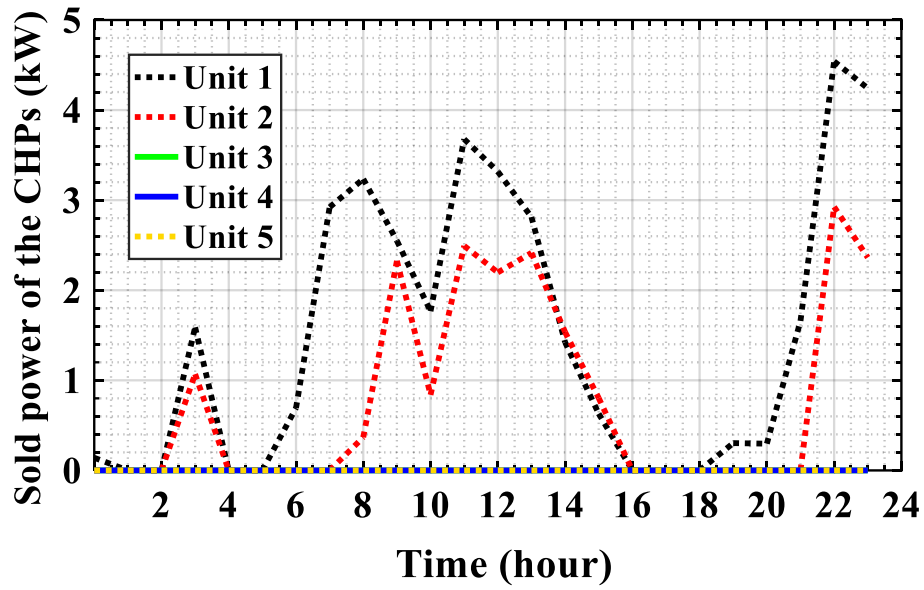


(b) Without coalition

Figure 16: The charging power of batteries in systems

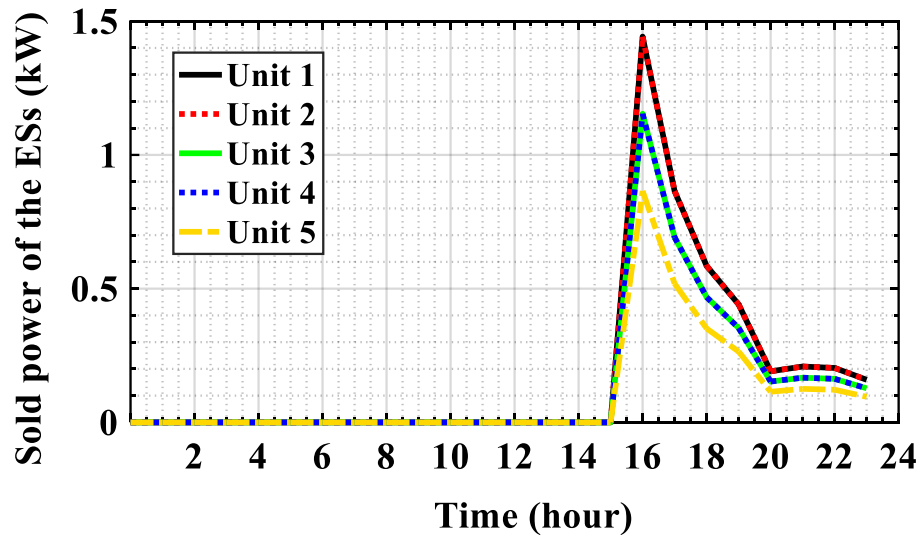


(a) With coalition

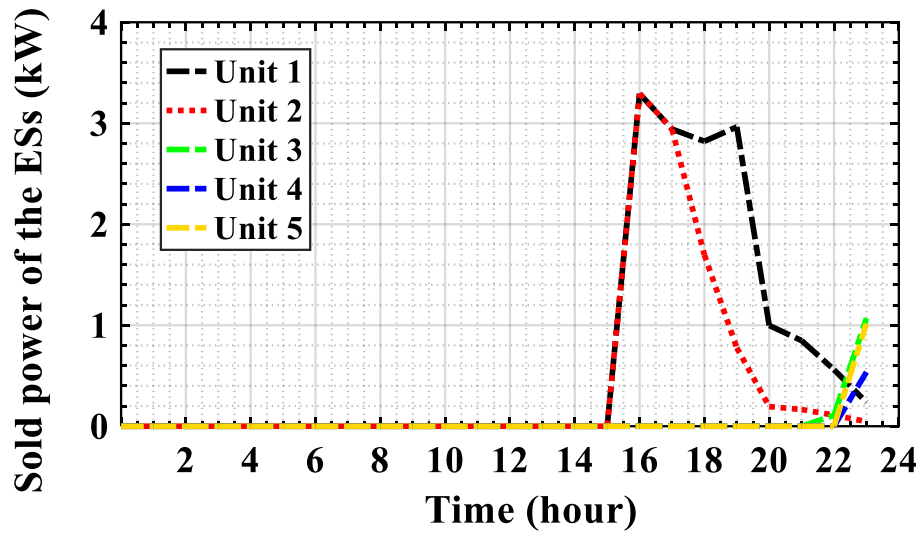


(b) Without coalition

Figure 17: The amount of power sold by CHP's in systems



(a) With coalition



(b) Without coalition

Figure 18: The amount of power sold by batteries in systems

Table 4: Charging and discharging power of EV's. in the non-coalition system.

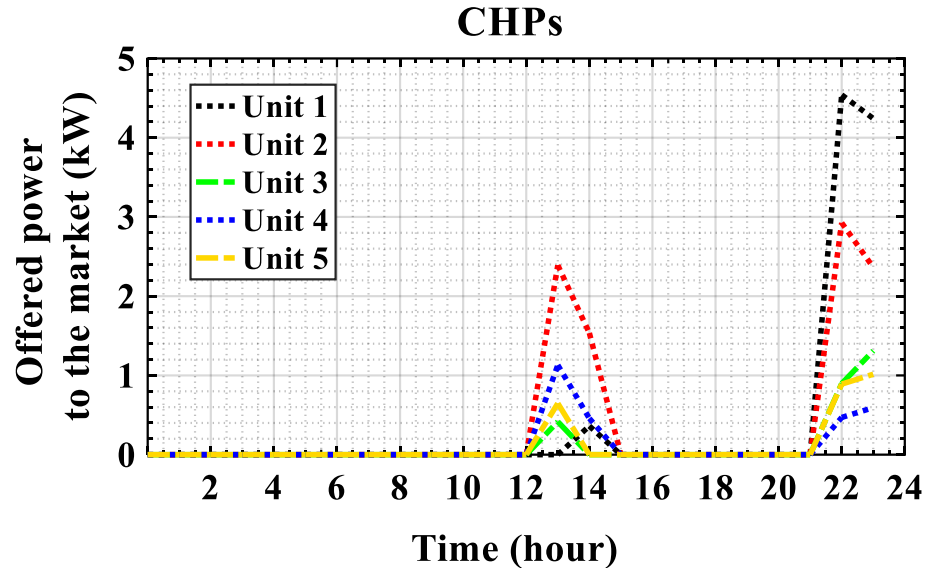
Unit/ hour	1 (kW)	2 (kW)	3 (kW)	4 (kW)	5 (kW)
1 to 3	3	3	3	3	3
4 to 16	0	0	0	0	0
17	-1.5	-1.1	-1.5	-1.5	-1.5
18	-3	-3	-3	-3	-3
19	0	-0.4	0	0	0
20 to 24	0	0	0	0	0

this case is particularly seen more in the coalition systems. Figure 21 shows that the offering price to the market is always lower than the market-clearing price (MCP). It is noted that the offering price curve is very similar to the trend of Figure 4.

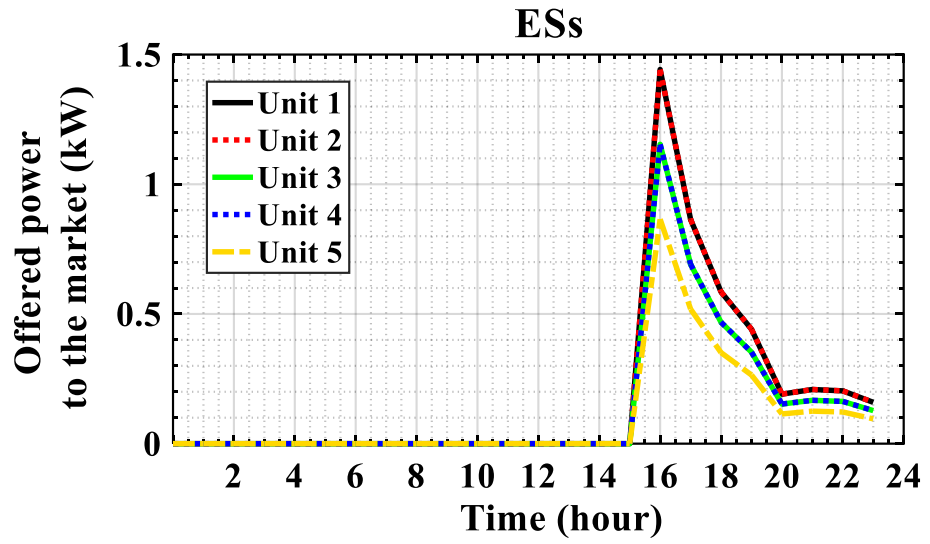
State of charge (SOC) and energy of storage's for systems with and without coalition are shown in Figures 22 and 23, respectively. According to Figures 22 and 23, at the end of the operation interval, the energy of storage's is almost used. In addition, the charging of batteries is performed at the off-peak hours and the discharging mode is performed at the peak load hours that increase the reliability in supplying the load and reduces the cost of the system.

Figure 24 shows the performance of CHP's with and without coalition modes. The total generation of CHP's for systems with and without coalition is calculated as 648.84kWh and 634.02kWh, respectively, which indicates that the CHP's have higher performance in the coalition mode. In addition, the total amount of energy purchased from the network with and without coalition modes are calculated as 1.5kWh and 58.69kWh, respectively. Clearly, the coalition system purchases less energy from the network which in turn improves the reliability, reduces cost and improves voltage stability of the network.

The amount of thermal energy generated by CHP's with and without coalition modes are shown in Figure 25. As seen, CHP's have more generation in the coalition

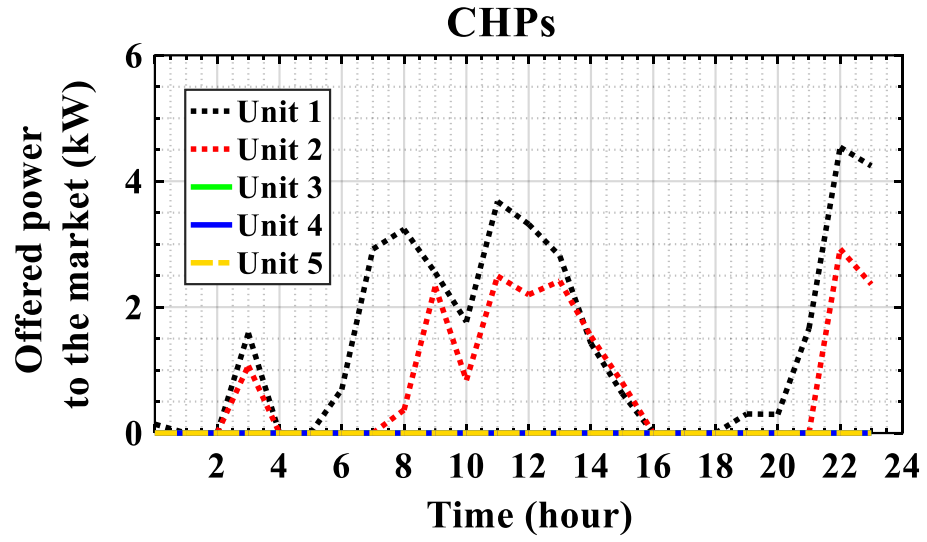


(a) CHP

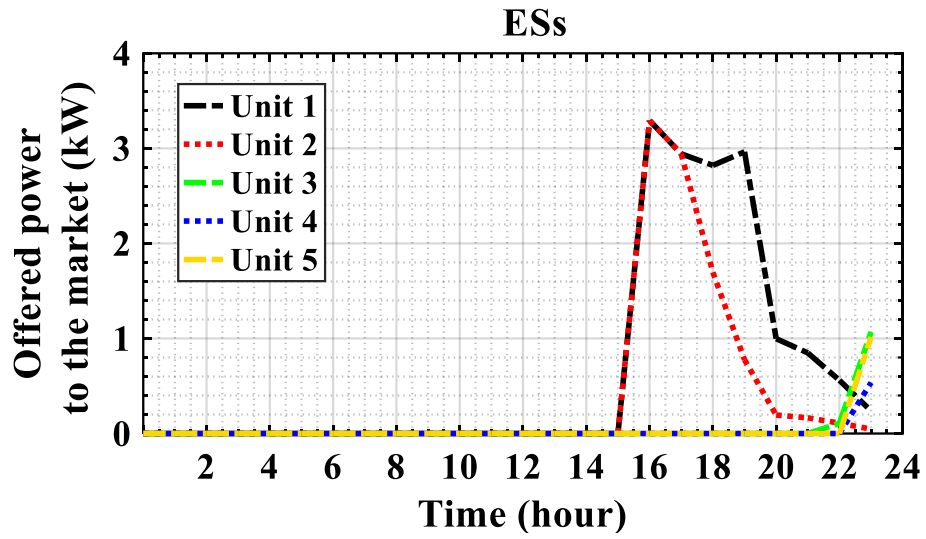


(b) storage's

Figure 19: Offered power by the units to the market



(a) CHP



(b) storage's

Figure 20: Offered power by the units to the market in the non-coalition system

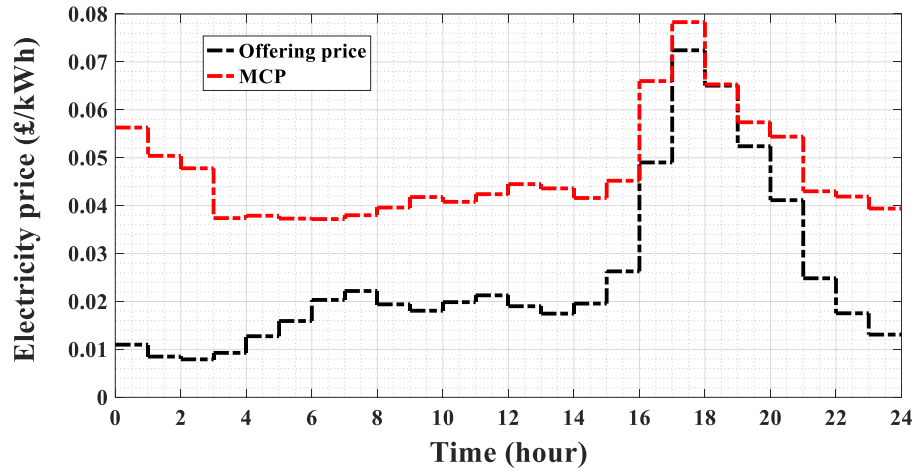


Figure 21: H-MG offering price to the market in comparison with market price

531 system and thermal power shortage in systems with and without coalition are cal-
532 culated equal as 189.76kWh and 207.19 kWh, respectively. Therefore, more gener-
533 ation of CHP's compensates the thermal and electrical power shortage, as the main
534 advantages of the coalition system. The amount of thermal power exchange be-
535 tween units is shown in Figure 26. After exchanging thermal power between units,
536 the total thermal shortage in the coalition system has been obtained as 169.34 kWh
537 that is 10.76% less than the results of the previous step. It is noted that at this step
538 the amount of thermal shortage in non-coalition mode is not changed.

539 The optimal utilization of CHP's reduces the dependency on the upstream net-
540 work and increases reliability in the thermal and electrical power supply leads to
541 deploying the optimum capacity of storage's. The unused capacity of CHP's is de-
542 picted in Figure 27. As seen, in the coalition system, the residual capacity of CHP's
543 is significantly lower.

544 The boilers generation and exchanged power between units are shown in Fig-
545 ures 28 and 29. The total generation of boilers and the thermal shortage with and
546 without coalition are 160.90 kWh and 188.31 kWh, and 0 kWh and 18.87 kWh,
547 respectively. Therefore, the coalition system has better performance. The next step
548 "supplying load from storage's" is not performed due to complete satisfaction of

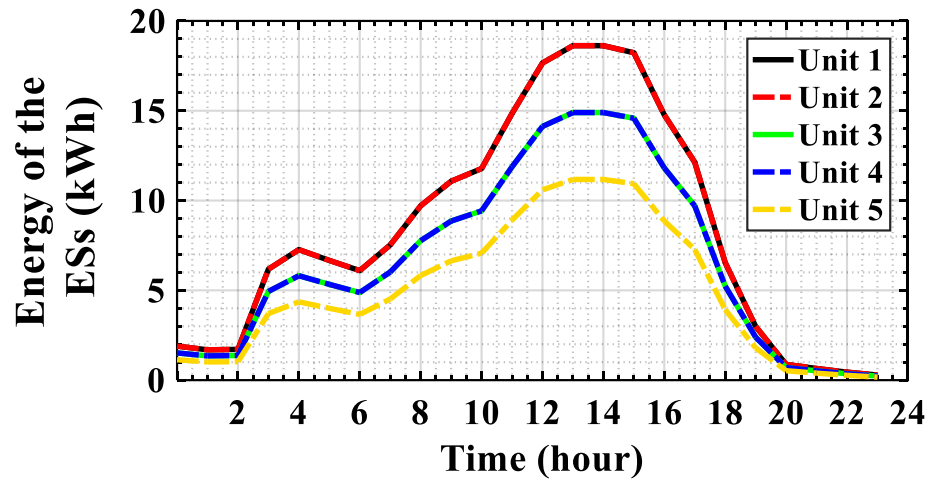
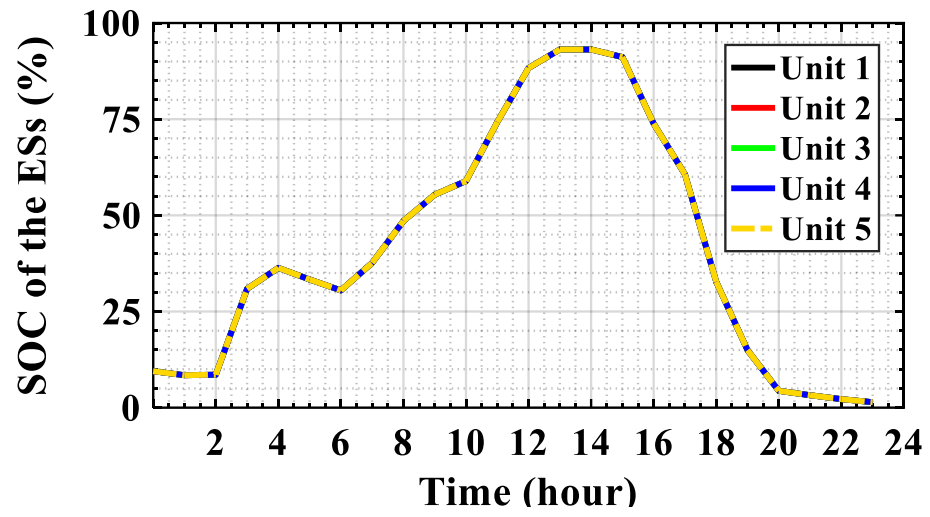
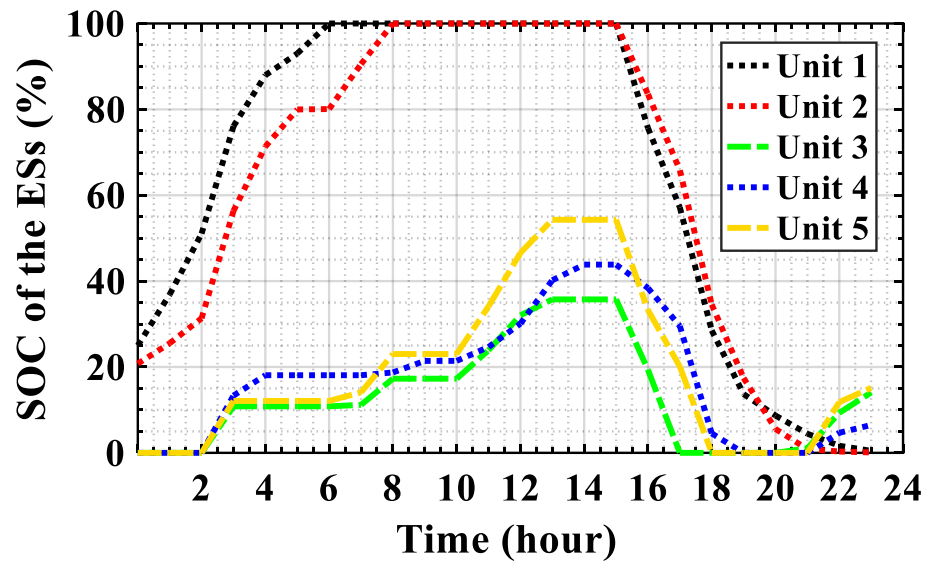
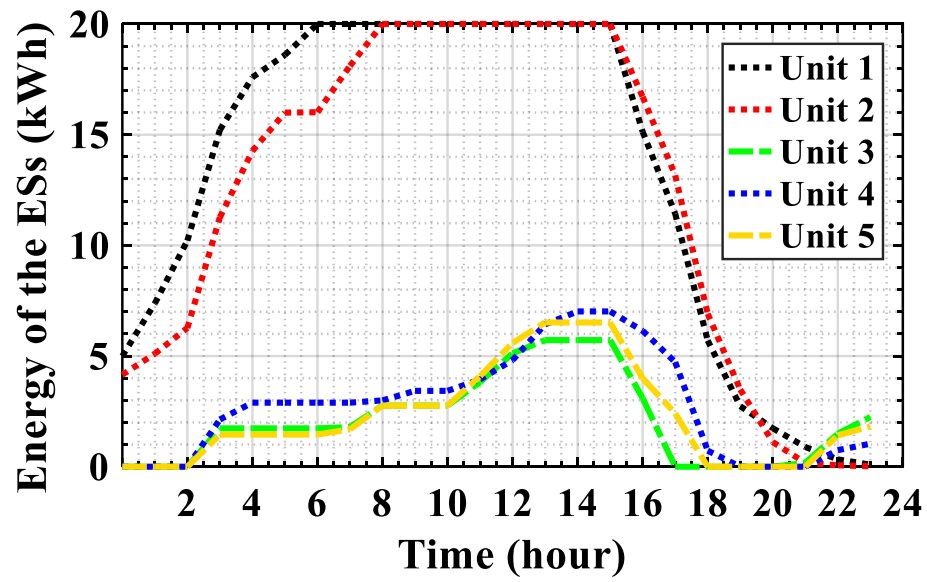


Figure 22: SOC and energy of units in the coalition system

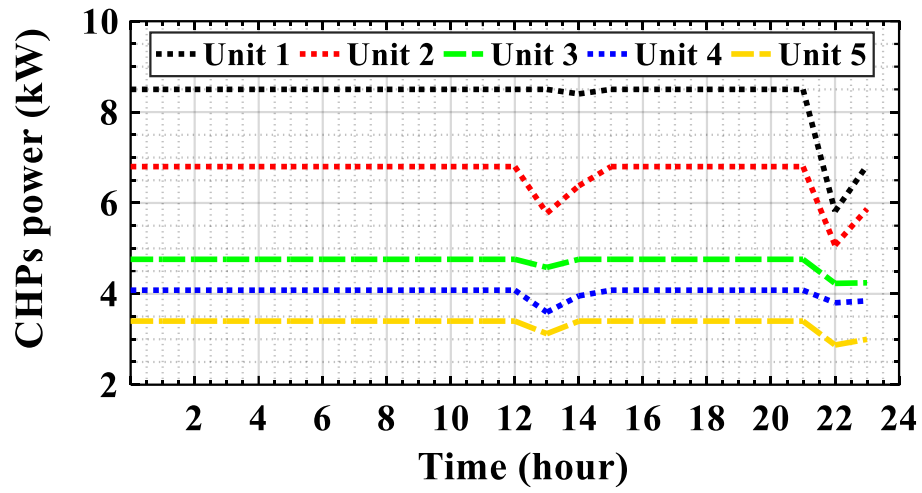


(a) SOC

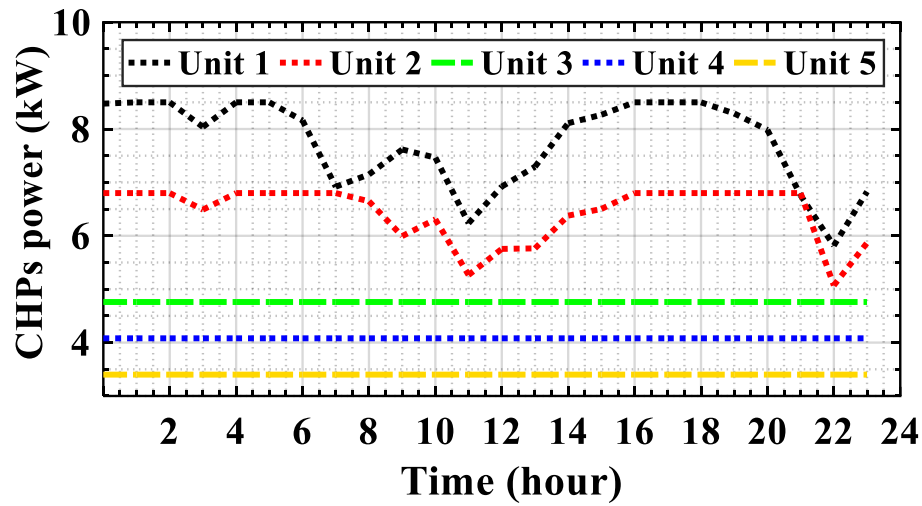


(b) Energy

Figure 23: SOC and energy of units in the non-coalition system

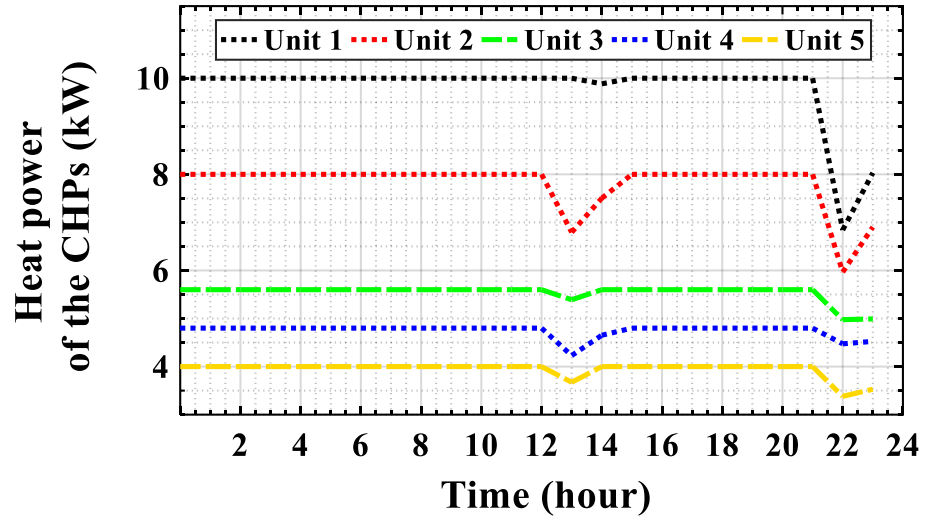


(a) Wit coalition

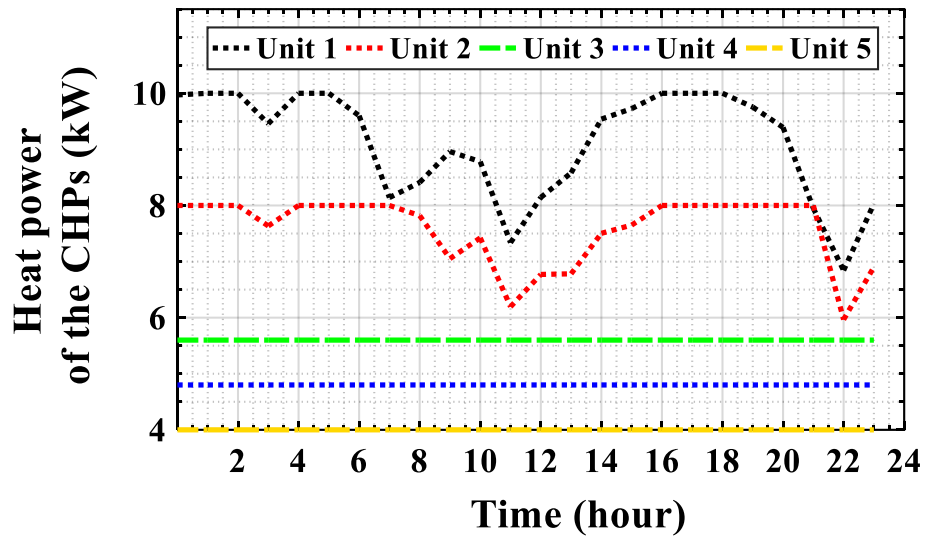


(b) Without coalition

Figure 24: The function of CHP's in systems

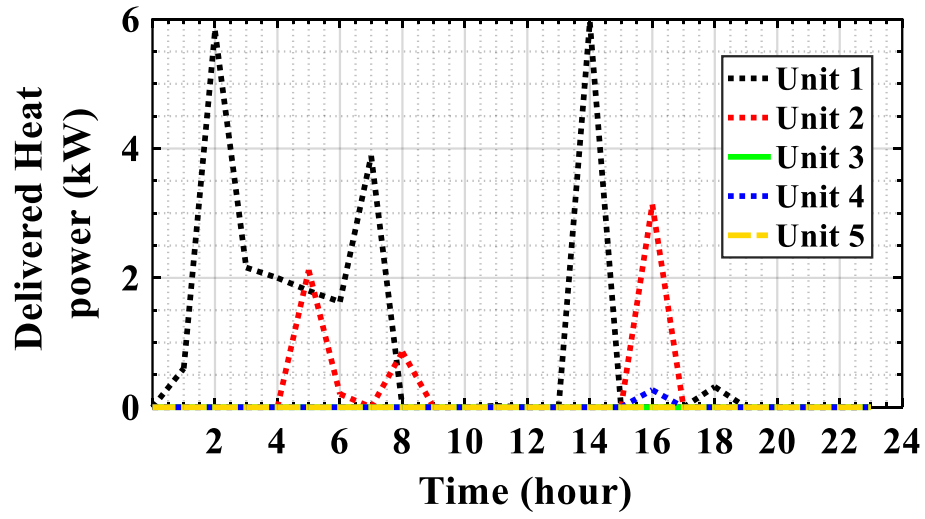


(a) Wit coalition

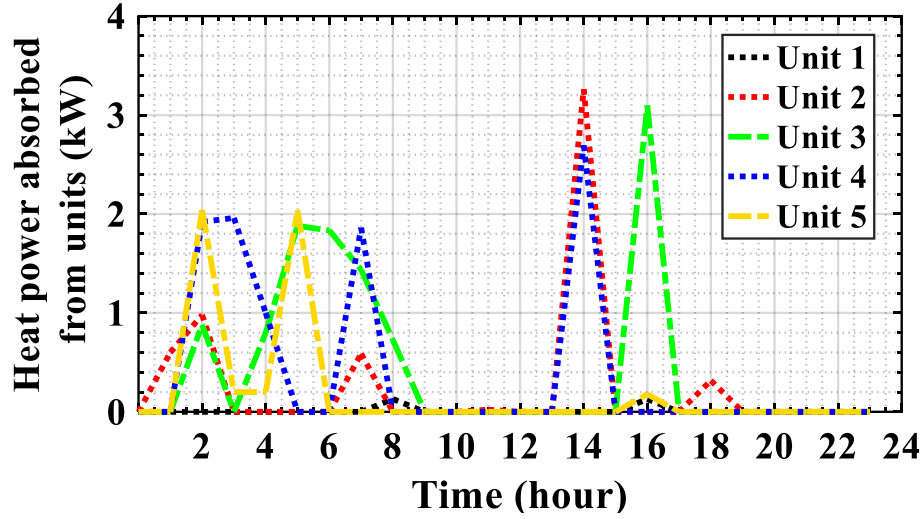


(b) Without coalition

Figure 25: The amount of thermal energy generated by CHP's

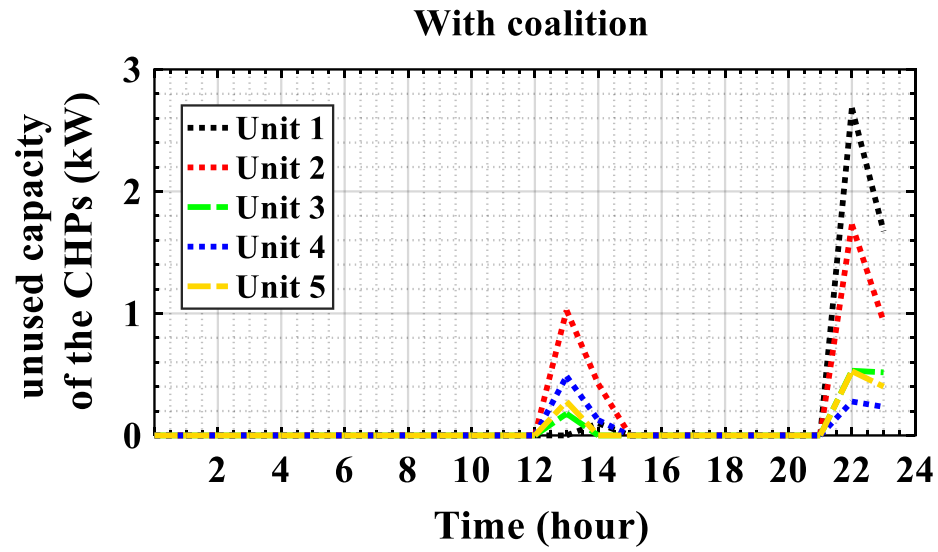


(a) Delivered thermal heat power

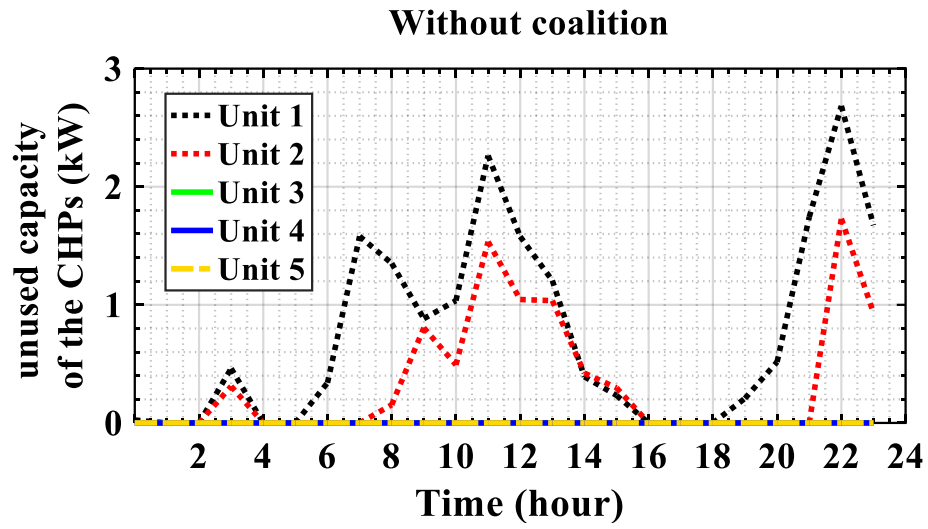


(b) Absorbed thermal heat power

Figure 26: Delivered and absorbed thermal heat power by units in the coalition system.



(a) With coalition

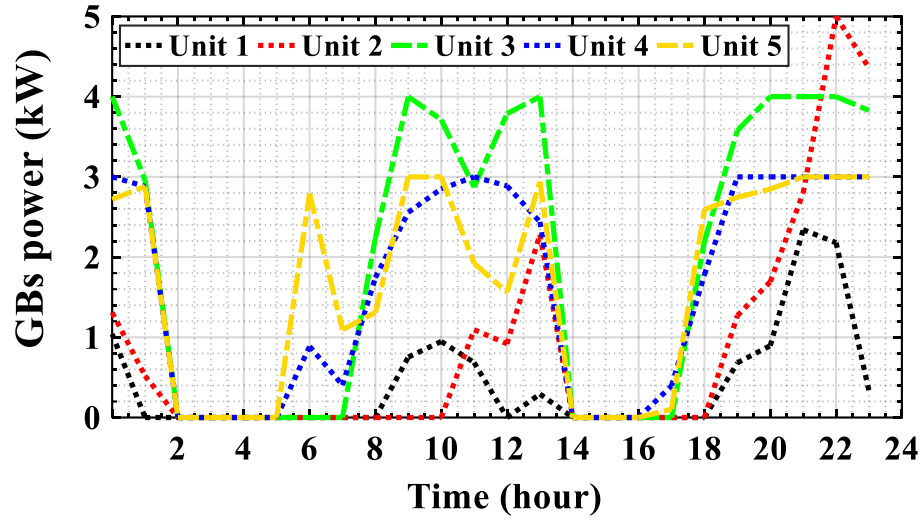


(b) Without coalition

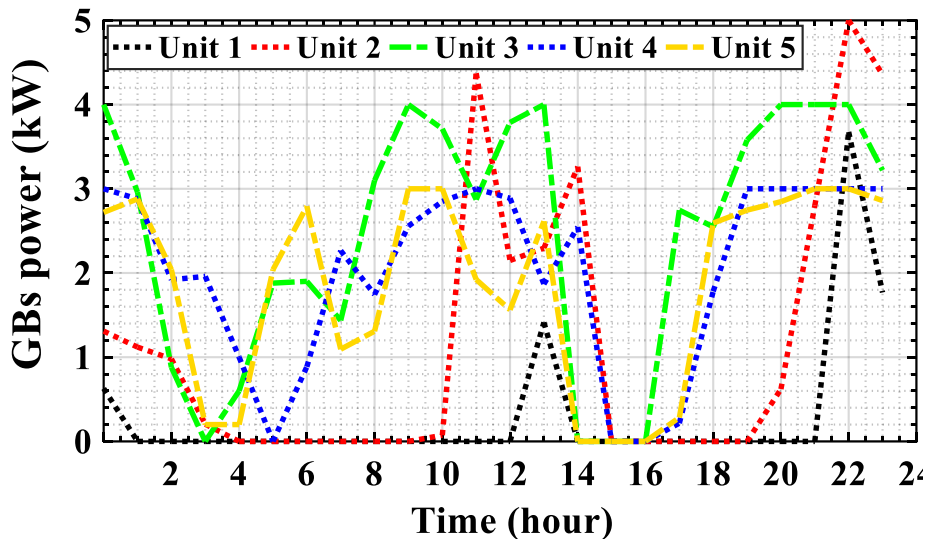
Figure 27: Unused capacity of CHP's for systems

549 thermal load. Dumped power is zero for both systems. The total cost of the system
550 with and without a coalition is £23.95 and £25.60, respectively, indicating 6.644%
551 of economic savings.

552 Summary of the results of Figures 7 to 29 and Tables 1 to 4 are illuminated as in
553 Table 5. As seen, the storage's have been able to receive more energy from the CHP's
554 due to the distribution of additional power between all storage's. According to items
555 3, 4, 8, 9 and 12, storage's have higher selling, charging/discharging efficiency.
556 Plus, according to items 5 and 6, charging/discharging is operated based on a smart
557 mechanism. The storage's are fully charged during the day and are not needed to
558 be recharged at peak hours. According to item 7, the discharge rate in the coalition
559 system is considered higher value due to the use of all storage's for discharging
560 proportion considering rated power. The results of the table show that the average
561 SOC of the storage's and total injected power to the H-MG, total sales efficiency, total
562 applied efficiency and generated electrical/thermal power of the CHP's is higher in
563 the coalition formation system. In addition, the amount of purchased power from
564 the main grid, primary heat shortage, total heat shortage, and cost of the system
565 is significantly lower in coalition formation systems. Items 25 and 26 to 28 are
566 related to the effect of thermal power exchange between units in heat shortage
567 and performance of GB's, respectively. The results show that, by exchanging of
568 thermal power, the shortage rate is significantly reduced, the GB's generate less
569 power and impose less cost on the system. Also, according to items 32 and 33, the
570 EV's participation in high price hours is higher in the coalition system, leading to
571 lower costs. Totally, the results of Table 5 demonstrate the priority of the proposed
572 method for the coalition-formation of residential complexes.

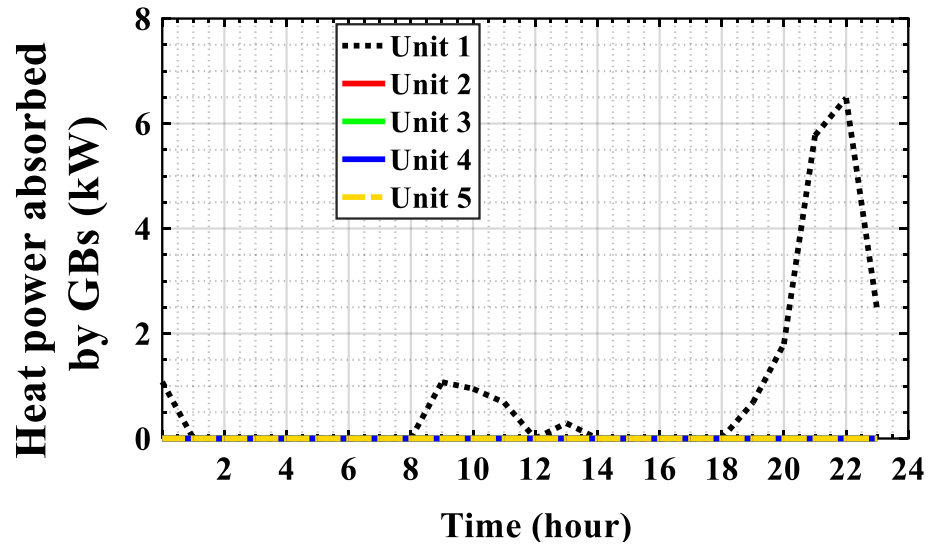


(a) With coalition

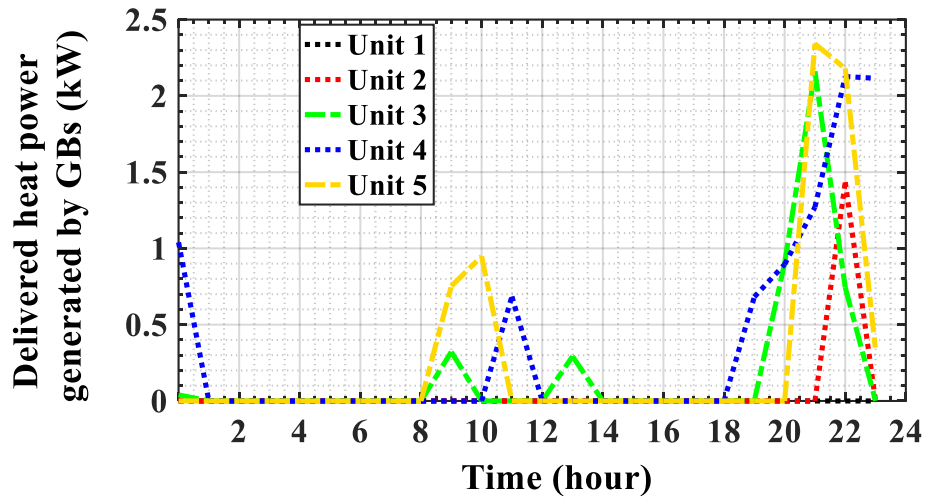


(b) Without coalition

Figure 28: The heat power generation of GBs in systems



(a) Absorbed heat power



(b) Delivered heat power

Figure 29: Absorbed and delivered heat power between units through GBs in the coalition system.

Table 5: Summarization of the results in the with and without coalition systems

item	Parameter	With coalition	Without coalition
1	Total remaining capacity of CHP's (after Steps 6 and Steps 7 of part A in Section 4.1 (kWh)	122.30	149.14
2	Total charging of electric storage's (ESs) from CHP's (kWh)	84	67.08
3	Charging efficiency of the ESs (from CHP's) (%)	$\frac{84}{122.3} \times 100 = 68.683$	$\frac{67.08}{149.14} \times 100 = 44.977$
4	Charging efficiency of ESs to total capacity (when charging CHP's) (%)	$\frac{84}{84} \times 100 = 100$	$\frac{67.08}{84} \times 100 = 79.857$
5	The total charging rate of ESs during peak and night hours (kWh)	7.83329	
6	Intelligent energy distribution between ESs proportions to nominal power (%)	100	0
7	The total energy discharged by ESs in the H-MG system (kWh)	65.6	35.25
8	The efficiency of the injected energy by ESs to H-MG system compared to available energy (%)	$\frac{65.6}{84} \times 100 = 78.095$	$\frac{35.25}{67.08} \times 100 = 52.549$
9	The efficiency of the injected energy by ESs to H-MG system compared to available total capacity (%)	$\frac{65.6}{84} \times 100 = 78.095$	$\frac{35.25}{84} \times 100 = 41.964$
10	Total remaining capacity of the ESs for sale to the grid (kWh)	18.4	31.83
11	The total energy sold to the grid by ESs (kWh)	17.202	26.613
12	Energy Efficiency Sold to the Grid by ESs (%)	$\frac{17.202}{18.4} \times 100 = 93.489$	$\frac{26.613}{31.83} \times 100 = 83.609$
13	Average SOC of the ESs (%)	93.12	66.76
14	the total energy injected by CHP's to H-MG system (kWh)	622.654	578.898
15	Total remaining capacity of CHP's for sale to the network (kWh)	38.305	82.061
16	Total energy sold to the grid by CHP's (kWh)	26.186	55.130
17	The efficiency of total energy sold to the grid by CHP's (kWh)	$\frac{26.186}{38.305} \times 100 = 68.361$	$\frac{55.130}{82.061} \times 100 = 67.181$
18	Total electrical power generated by CHP's (kWh)	648.841	634.028
19	Applied efficiency of CHP's in the H-MG system (%)	$\frac{648.841}{660.96} \times 100 = 98.166$	$\frac{634.028}{660.96} \times 100 = 95.925$
20	Total thermal energy generated by CHP's (kWh)	763.361	745.934
21	The total electrical power purchased from the grid (kWh)	1.5	58.69
22	Improvement in the amount of electricity purchased from the grid (%)	97.444	-
23	The total thermal shortage after Step 1 of part B in Section 4.1 (kWh)	189.76	207.19
24	The total thermal shortage after Step 1 of part B in Section 4.1 and exchange thermal power between units (kWh)	172.62	207.19
25	The rate of improvement in thermal shortage after Step 2 of part B in Section 4.1 (%)	9.027	0
26	Total generation of GBs in their own units (kWh)	151.36	188.31
27	Total generation of GBs in other units (kWh)	21.26	0
28	Improvement rate in thermal power shortage after heat exchange between units by GBs (%)	100	0
29	The total shortage of thermal power (kWh)	0	18.87
30	Total Cost (£)	23.95	25.60
31	Amount of cost improvement after adding coalition to H-MG system (%)	6.445	-

573 5.3. Single H-MG with Coalition and Stochastic Load

574 The second part of simulations aims to examine different types of loads and
575 their effects on the results. In this regard, 31 different types of thermal and electrical
576 loads are selected to cover different aspects of the examination. In order to generate
577 these load profiles, different characteristics of load such as peak hours, off-peak
578 hours, peak size, average and variance of load have been changed stochastically.
579 The simulation results of these loads are shown in Table 6.

580 According to Table 6, it is clear that the coalition system has better performance
581 in terms of cost, electrical and thermal ENS and thermal dumped energy. If these
582 31 load profiles are considered as the load profile of 31 days of one month, the to-
583 tal cost, electrical and thermal ENS and thermal dumped energy will be improved
584 by 6.248%, 80.6073%, 99.9657%, and 100%, respectively, as compared to non-
585 coalition system. As a result, using the coalition system improves the performance
586 of H-MG, which indicates the high efficiency of the proposed algorithm for the coali-
587 tion system.

Table 6: Results of “stochastic scheduling” in systems with and without coalition.

Load number	Coalition system				Without coalition system						Amount of improvement		
	Cost (£)	Electrical ENS (kWh)	Thermal ENS (kWh)	Thermal damp (kWh)	Thermal backup (kWh)	Cost (£)	Electrical ENS (kWh)	Thermal ENS (kWh)	Thermal damp (kWh)	Cost (£)	Electrical ENS (%)		
1	23.953	1.505	0	0	0	25.606	58.693	-18.879	0	6.456	97.436		
2	24.44	2.319	0	0	0	26.62	67.691	-23.819	5.591	8.189	96.574		
3	24.863	0	-0.341	0	3.874	26.287	57.612	-80.607	0	5.417	100		
4	25.858	6.578	0	0	0	27.198	66.566	-35.155	0	4.927	90.118		
5	25.45	0.967	0	0	0	26.814	41.644	-16.244	0	5.087	97.678		
6	25.86	7.176	0	0	0	27.29	70.162	-25.705	0	5.24	89.772		
7	25.853	4.234	0	0	0	27.151	40.042	-13.695	0	4.781	89.426		
8	25.51	0.807	0	0	0	26.638	58.421	-27.753	0	4.235	98.619		
9	26.301	18.574	0	0	0	27.765	76.7	-38.589	0	5.273	75.784		
10	24.982	0.291	0	0	0	26.461	84.031	-45.631	0	5.589	99.654		
11	25.736	1.962	0	0	0	27.049	66.087	-30.085	3.681	4.854	97.031		
12	32.438	138.121	0	0	0	33.654	186.527	-39.533	10.628	3.613	25.951		
13	32.38	138.121	0	0	0	33.985	184.147	-36.397	9.683	4.723	24.994		
14	24.65	4.042	0	0	0	26.989	83.833	-39.468	0	8.666	95.179		
15	24.737	6.878	0	0	0	26.67	74.987	-35.115	0	7.248	90.828		
16	24.97	4.102	0	0	0	27.113	65.477	-26.221	0	7.904	93.735		
17	25.173	8.598	0	0	0	26.697	57.369	-21.774	0	5.709	85.013		
18	25.114	4.122	0	0	0	26.898	46.827	-22.146	0	6.632	91.197		
19	25.095	8.426	0	0	0	26.671	42.214	-15.844	0	5.909	80.04		
20	24.938	4.602	0	0	0	26.949	64.2	-43.128	0	7.462	92.832		
21	24.581	7.942	0	0	0	26.505	62.104	-25.862	0	7.259	87.212		
22	25.479	3.806	0	0	0	27.514	52.19	-14.702	0	7.396	92.707		
23	25.448	10.222	0	0	0	26.932	43.313	-12.296	0	5.51	76.4		
24	25.55	4.666	0	0	0	26.465	55.809	-28.374	0	3.457	91.639		
25	24.728	7.758	0	0	0	26.312	53.768	-23.598	0	6.02	85.571		
26	24.354	4.606	0	0	0	26.374	73.053	-43.03	0	7.659	93.695		
27	24.316	6.51	0	0	0	26.21	70.101	-37.172	0	7.226	90.713		
28	24.53	4.586	0	0	0	26.683	88.387	-41.707	0	8.069	94.811		
29	24.469	6.262	0	0	0	26.375	82.939	-38.772	0	7.227	92.45		
30	24.759	4.106	0	0	0	27.298	71.509	-29.1	2.864	9.301	94.258		
31	24.848	6.694	0	0	0	26.93	63.578	-24.67	0	7.731	89.471		
Total:	791.363	428.583	-0.341	0	3.874	844.103	2209.981	-995.071	32.447	-	-	-	-

588 5.4. H-MG's with coalition on Large Networks

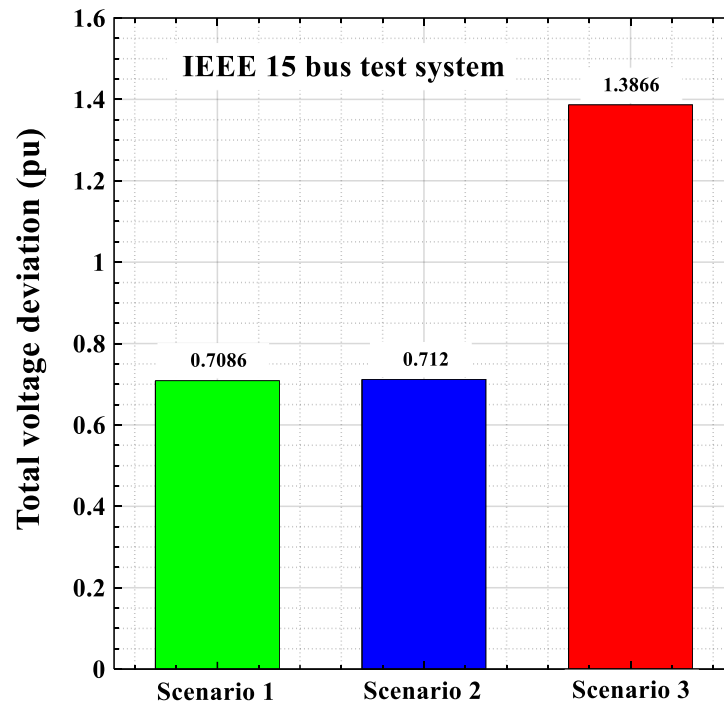
589 In the last part of the analysis, the effect of the application of **the** coalition system
590 on the voltage quality of large-scale 15 and 33-bus networks, and on reliability
591 indices during fault occurrence, **are** investigated. The evaluations are conducted
592 based on the assumption of having an identical load profile for all buses. In this
593 regard, the above-mentioned loads and H-MG's are present **for** all buses.

594 Firstly, the impact of “systems with and without coalition” and “ordinary system
595 without **H-MG**” on voltage deviation of the distribution network are studied. To
596 assess the voltage deviation of the network, three different scenarios are considered
597 for load combination, **according to section 3.7. part A**. The simulation results of 15
598 and 33-bus networks are presented in Figure 30.

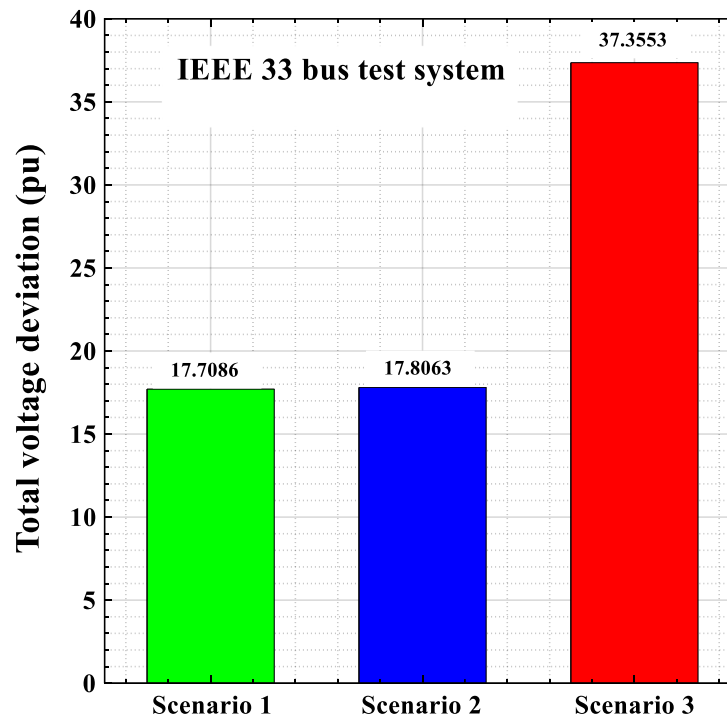
599 Figure 30 demonstrates that when “loads with **the** coalition” are present in the
600 system, the voltage deviation of the network is lower as compared to other scenar-
601 ios. **The results of the first and second scenarios are similar, but they are different**
602 **from the results of the third scenario. These results indicate the presence of H-MG's,**
603 **especially with the coalition system, in the network is effective and helps to reduce**
604 **voltage deviation**. According to Figure 30, by increasing the size of the network, the
605 positive effect of “MG's with coalition” is highlighted. The voltage deviation of the
606 network in **the** modes of “MG's with **the** coalition” and “MG's without coalition” is
607 improved by 95.68% and 94.74% in the 15-bus system, and 110.95% and 109.78%
608 in the 33-bus system, respectively. Therefore, the application of H-MG's, especially
609 with the coalition, on large scales can be highly useful.

610 In order to study the impact of the presence of “systems with and without coali-
611 tion” and “systems without **the H-MG**” on the reliability of the distribution network,
612 the occurrence of faults in the 15 and 33-bus test systems, is considered. The ENS
613 and **the** number of dissatisfied customers (NODC) are the main reliability assess-
614 ment factors that **is** selected in this paper.

615 The occurrence of a fault in the 15-bus system is performed according to Fig-
616 ure 31. In this regard, **firstly**, a fault is placed in line 9 (**Step 1**). Then, the relay 9
617 operates and disconnects the faulty line from the network (**Step 2**). Next, the re-
618 configuration is carried out and line 13 is connected (**Step 3**). It is assumed that the



(a) Standard IEEE 15-bus



(b) Standard IEEE 33-bus

Figure 30: The voltage deviation of standard IEEE a) 15 and b) 33-bus test systems under three load scenarios.

reconfiguration occurs half an hour after the fault takes place. Therefore, the buses 9, 10 and 11 remain disconnected for half an hour and two hours in the presence and absence of reconfiguration, respectively [38–42] In the 33-bus test system, a fault is placed between bus 12 and 13. Then, the relay next to bus 12 operates and removes the fault. It is assumed that it will take 2 hours to fix the line, so the buses 13-18 will be disconnected for 2 hours. Similar to voltage deviation analysis, three types of load scenarios are considered and the results for 15 and 33-bus systems are provided in Tables 7 and 8.

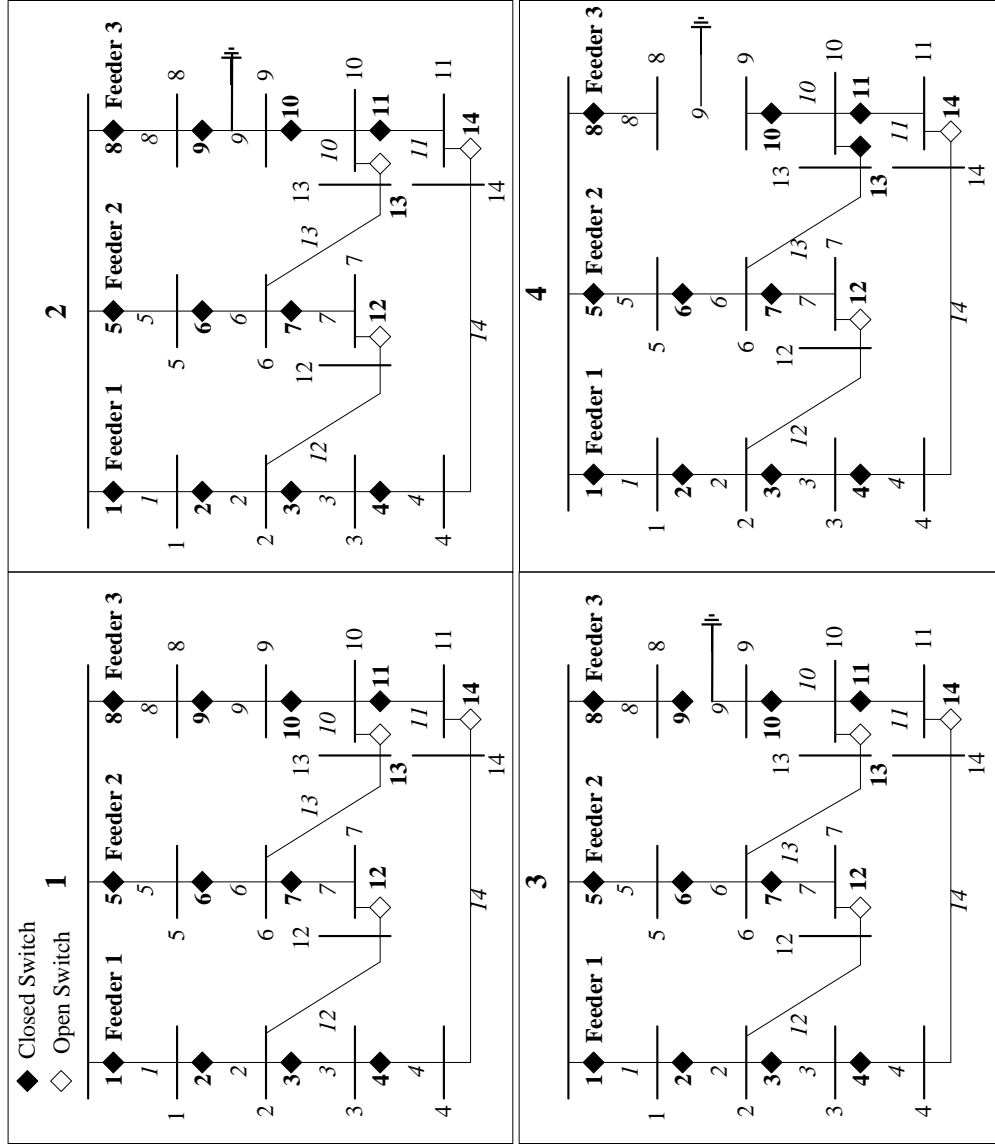


Figure 31: The effect of the coalition system on the reliability in the standard IEEE 15-bus network.

Table 7: The ENS and NODC results of the IEEE 15-bus system in the presence of reconfiguration.

	1 st type of loads		2 nd type of loads		3 rd type of loads		Total	
	NODC	ENS	NODC	ENS	NODC	ENS	NODC	ENS
Scenario 1	0	0	6.6114	6	41.928	15	48.5394	21
Scenario 2	-	-	13.2228	12	41.928	15	55.1508	27
Scenario 3	-	-	-	-	125.784	45	125.784	45

Table 8: The ENS and NODC results of the IEEE 33-bus system in the different load scenarios.

	1 st type of loads		2 nd type of loads		3 rd type of loads		Total	
	NODC	ENS	NODC	ENS	NODC	ENS	NODC	ENS
Scenario 1	18.597	12	58.4004	24	365.2032	60	442.2006	96
Scenario 2	-	-	116.8008	48	365.2032	60	482.004	108
Scenario 3	-	-	-	-	1095.6096	180	1095.6096	180

According to the results of Tables 7 and 8, it is clear that the results of scenario 1 are better than other scenarios. As seen in Table 8, the ENS and NODC are improved by 9.0012% and 12.5% in the system with the coalition as compared to the system without a coalition, and 147.763% and 87.5% in the system with the coalition as compared to the system without H-MG, respectively. The difference between scenarios 1 and 2 is that, in scenario 2, the coalition system is removed and the system without coalition is replaced, in order to prove the effectiveness of systems with the coalition. The results of Tables 7 and 8 show that the systems with coalition improve the ENS and NODC in the main grid. This also holds the same evaluation for scenarios 2 and 3, where removing “system with MG” increases ENS and NODC.

5.5. Sensitivity of the Proposed Method on the Problem Variables

According to Eq. 13, the impact of systems with the coalition is determined on each bus which is independent of the type of network and applicable to various networks. In this regard, Figures 30 and 31 and Tables 7 and 8 prove this claim. The reason is, when the number of systems with coalition in each bus increases, the power and current consumption in that bus decreases. As a result, voltage quality improves, while energy losses and dependency on the network are decreases. By decreasing the dependency on the network, reliability is improved. Therefore, if the connection between buses and the network is interrupted, the amount of ENS

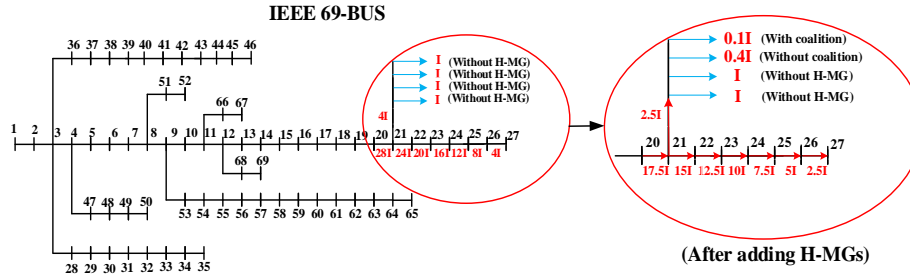


Figure 32: Schematic proof of coalition system performance on the IEEE 69-bus test system

is decreased. For example, according to Figure 32, suppose in the IEEE 69-bus test system, 4 residential complexes are on each bus. By adding coalition and non-coalition systems instead of non-home MG systems, the current absorption for each type of load was decreased by 90% and 60%, respectively. The current of the lines is shown in red, which are significantly decreased.

Problem variables include the network type, RESs, number of residential units, thermal and electrical dispatchable sources, storage and electrical and thermal loads. In this section, it was proved that the results are independent of the network type. Assuming so, changing these parts does not violate the validity of the proposed method considering the uncertainty of RESs. The results of Table 6 demonstrate that the proposed method is effective in all considered load cases. Moreover, the nature of the proposed method is not iterative. By changing the number of units, only a few loops are added to the method to calculate the optimal solutions. Therefore, with the change in load and number of units, the generality of the proposed method is not affected. Also, the capacity of thermal and electrical dispatchable sources and storage's is preselected according to the type of consumption of each unit and system. The capacity of this equipment cannot be adjusted more or less than calculated value as well as sensitivity analysis is not possible without changing other capacities. Since the generality of the proposed method is not affected by changing the variables of the problem, it can be concluded that the proposed method has sufficient robustness.

According to simulations, the efficiency of the proposed algorithm for the coal-

tion system in the studied H-MG has been tested on different loads types. It has been proved that when the proposed algorithm is applied, the system with coalition behaves better than the system without a coalition in terms of cost, energy loss, and reliability of the main grid. Finally, it has been proved that MG's with a coalition can be useful for both small- and large-scale systems and reduce the voltage deviation and increase reliability in the distribution system.

6. Conclusions

In the present study, the effect of coalition formation of units in H-MG's is investigated on different objectives and large-scales networks in terms of voltage quality and grid reliability. In the small-scale, an apartment building consisting of 5 units is considered that has electrical sources such as CHP's, solar panels, and WT's; and heat sources such as boilers and solar water heaters. To store electrical and thermal energy, batteries and thermal storage's are used. All units could exchange electrical and thermal power with together and with the main grid. In this paper, a technoeconomic multi-level optimization method is proposed by considering high-level technical constraints and policies to encourage players to participate in coalition formation. Also, functional methods are introduced for operation of EV's and electrical storage's, and power exchange of CHP's, GB's and thermal storage's between units. In addition, the excess power of the renewables, CHP's, and storage's is sold using the concept of "time-varying elasticity". The examinations are conducted in three general branches in MATLAB software. In Step 1, the efficiency of the proposed algorithm is proved for "H-MG with the coalition" for a typical load. Next, the robustness of the proposed method against load variation is investigated. According to the results, within a month, the coalition-formation system, improves the total cost, electrical and thermal ENS and thermal dumped energy as compared to the non-coalition system, 6.248%, 80.6073%, 99.9657%, and 100%, respectively. Finally, it is proved that "MG with the coalition" improves voltage quality and reliability of the network. Examinations are carried out on the IEEE 15 and 33-bus systems considering the effect of reconfiguration. The voltage deviation in the coalition and

697 non-coalition system are improved 95.68% and 94.74% in the 15-bus system, along
698 with 110.95% and 109.78% in the 33-bus system, respectively. Also, the ENS and
699 NODC are improved 9.0012 and 12.5% in the coalition system as compared to the
700 non-coalition system without home MG, and 147.763 and 87.5%, respectively. The
701 overall results indicate that the “system with the coalition” improves MG and net-
702 work performance in terms of the total cost, electrical and thermal ENS, thermal
703 dumped energy, voltage quality, and reliability indices.

7. Acknowledgments

This research was supported by the British council under grant contract No: IND/CONT/GA/18-19/22.

References

- [1] A. Pallante, L. Adacher, M. Botticelli, S. Pizzuti, G. Comodi, A. Monteriu, Decision support methodologies and day-ahead optimization for smart building energy management in a dynamic pricing scenario, *Energy and Buildings* 216 (2020) 109963.
- [2] H. J. Monfared, A. Ghasemi, A. Loni, M. Marzband, A hybrid price-based demand response program for the residential micro-grid, *Energy* 185 (2019) 274–285.
- [3] H. Mehrjerdi, R. Hemmati, Coordination of vehicle-to-home and renewable capacity resources for energy management in resilience and self-healing building, *Renewable Energy* 146 (2020) 568 – 579.
- [4] M. Marzband, E. Yousefnejad, A. Sumper, J. L. Domínguez-García, Real time experimental implementation of optimum energy management system in standalone microgrid by using multi-layer ant colony optimization, *International Journal of Electrical Power Energy Systems* 75 (2016) 265–274.

- [5] Z. Liang, D. Bian, X. Zhang, D. Shi, R. Diao, Z. Wang, Optimal energy management for commercial buildings considering comprehensive comfort levels in a retail electricity market, *Applied Energy* 236 (2019) 916–926.
- [6] A. Jafari, T. Khalili, H. G. Ganjehlou, A. Bidram, Optimal integration of renewable energy sources, diesel generators, and demand response program from pollution, financial, and reliability viewpoints: A multi-objective approach, *Journal of Cleaner Production* 247 (2020) 119100.
- [7] M. Marzband, H. Alavi, S. S. Ghazimirsaeid, H. Uppal, T. Fernando, Optimal energy management system based on stochastic approach for a home microgrid with integrated responsive load demand and energy storage, *Sustainable Cities and Society* 28 (2017) 256–264.
- [8] V. Aryanpur, M. S. Atabaki, M. Marzband, P. Siano, K. Ghayoumi, An overview of energy planning in iran and transition pathways towards sustainable electricity supply sector, *Renewable and Sustainable Energy Reviews* 112 (2019) 58–74.
- [9] T. Khalili, S. Nojavan, K. Zare, Optimal performance of microgrid in the presence of demand response exchange: A stochastic multi-objective model, *Computers Electrical Engineering* 74 (2019) 429–450.
- [10] H. R. Gholinejad, A. Loni, J. Adabi, M. Marzband, A hierarchical energy management system for multiple home energy hubs in neighborhood grids, *Journal of Building Engineering* 28 (2020) 101028.
- [11] X. Wu, X. Hu, X. Yin, S. J. Moura, Stochastic optimal energy management of smart home with pev energy storage, *IEEE Transactions on Smart Grid* 9 (3) (2018) 2065–75.
- [12] M. Ashouri, B. C. Fung, F. Haghighat, H. Yoshino, Systematic approach to provide building occupants with feedback to reduce energy consumption, *Energy* 194 (2020) 116813.

- [13] M. Marzband, S. S. Ghazimirsaeid, H. Uppal, T. Fernando, A real-time evaluation of energy management systems for smart hybrid home microgrids, *Electric Power Systems Research* 143 (2017) 624–33.
- [14] T. Molla, B. Khan, B. Moges, H. H. Alhelou, R. Zamani, P. Siano, Integrated optimization of smart home appliances with cost-effective energy management system, *CSEE Journal of Power and Energy Systems* 5 (2) (2019) 249–58.
- [15] R. Hao, Q. Ai, T. Guan, Y. Cheng, D. Wei, Decentralized price incentive energy interaction management for interconnected microgrids, *Electric Power Systems Research* 172 (2019) 114–28.
- [16] M. Marzband, F. Azarinejadian, M. Savaghebi, E. Pouresmaeil, J. M. Guerrero, G. Lightbody, Smart transactive energy framework in grid-connected multiple home microgrids under independent and coalition operations, *Renewable Energy* 126 (2018) 95–106.
- [17] M. Marzband, M. Javadi, J. L. Domínguez-Garcá, M. M. Moghaddam, Non-cooperative game theory based energy management systems for energy district in the retail market considering der uncertainties, *IET Generation, Transmission Distribution* 10 (12) (2016) 2999–3009.
- [18] M. Marzband, R. R. Ardeshiri, M. Moafi, H. Uppal, Distributed generation for economic benefit maximization through coalition formation-based game theory concept, *International Transaction on electrical energy systems* 27 (6) (2017) 1–20.
- [19] M. Marzband, M. Javadi, S. A. Pourmousavi, G. Lightbody, An advanced retail electricity market for active distribution systems and home microgrid interoperability based on game theory, *Electric Power Systems Research* 157 (2018) 187–199.
- [20] M. Marzband, M. H. Fouladfar, M. F. Akorede, G. Lightbody, E. Pouresmaeil, Framework for smart transactive energy in home-microgrids consid-

- ering coalition formation and demand side management, *Sustainable Cities and Society* 40 (2018) 136–54.
- [21] F. Brahman, M. Honarmand, S. Jadid, Optimal electrical and thermal energy management of a residential energy hub, integrating demand response and energy storage system, *Energy and Buildings* 90 (2015) 65–75.
 - [22] M. A. Mirzaei, M. Nazari-Heris, B. Mohammadi-Ivatloo, K. Zare, M. Marzband, A. Anvari-Moghaddam, A novel hybrid framework for co-optimization of power and natural gas networks integrated with emerging technologies, *IEEE Systems Journal* (2020) 1–11.
 - [23] T. Adefarati, R. Bansal, Reliability, economic and environmental analysis of a microgrid system in the presence of renewable energy resources, *Applied Energy* 236 (2019) 1089–114.
 - [24] T. Khalili, A. Jafari, M. Abapour, B. Mohammadi-Ivatloo, Optimal battery technology selection and incentive-based demand response program utilization for reliability improvement of an insular microgrid, *Energy* 169 (2019) 92–104.
 - [25] N. Ghorbani, A. Kasaeian, A. Toopshekan, L. Bahrami, A. Maghami, Optimizing a hybrid wind-pv-battery system using ga-pso and mopso for reducing cost and increasing reliability, *Energy* 154 (2018) 581–591.
 - [26] S. Singh, S. Jagota, M. Singh, Energy management and voltage stabilization in an islanded microgrid through an electric vehicle charging station, *Sustainable Cities and Society* 41 (2018) 679–694.
 - [27] T. Khalili, M. T. Hagh, S. G. Zadeh, S. Maleki, Optimal reliable and resilient construction of dynamic self-adequate multi-microgrids under large-scale events, *IET Renewable Power Generation* 13 (10) (2019) 1750–60.
 - [28] A. Jafari, H. Ganjeh Ganjehlou, F. Baghal Darbandi, B. Mohammadi-Ivatloo, M. Abapour, Dynamic and multi-objective reconfiguration of distribution network using a novel hybrid algorithm with parallel processing capability, *Applied Soft Computing* 90 (2020) 106146.

- [29] Weather in london, england, united kingdom n.d., Available at: https://www.cableizer.com/tools/solar_radiation/, [accessed April 16, 2020].
- [30] M. Nazari-Heris, M. A. Mirzaei, B. Mohammadi-Ivatloo, M. Marzband, S. Asadi, Economic-environmental effect of power to gas technology in coupled electricity and gas systems with price-responsive shiftable loads, *Journal of Cleaner Production* 244 (2020) 118769.
- [31] M. Marzband, M. Ghadimi, A. Sumper, J. L. Domínguez-García, Experimental validation of a real-time energy management system using multi-period gravitational search algorithm for microgrids in islanded mode, *Applied Energy* 128 (2014) 164–74.
- [32] J. Abushnaf, A. Rassau, W. Górniewicz, Impact of dynamic energy pricing schemes on a novel multi-user home energy management system, *Electric Power Systems Research* 125 (2015) 124–32.
- [33] N. Gholizadeh, G. Gharehpetian, M. Abedi, H. Nafisi, M. Marzband, An innovative energy management framework for cooperative operation management of electricity and natural gas demands, *Energy Conversion and Management* 200 (2019) 112069.
- [34] N. V. Kovački, P. M. Vidović, A. T. Sarić, Scalable algorithm for the dynamic reconfiguration of the distribution network using the lagrange relaxation approach, *International Journal of Electrical Power Energy Systems* 94 (2018) 188–202.
- [35] A. Jafari, H. Ganjeh Ganjehlou, T. Khalili, B. Mohammadi-Ivatloo, A. Bidram, P. Siano, A two-loop hybrid method for optimal placement and scheduling of switched capacitors in distribution networks, *IEEE Access* 8 (2020) 38892–38906.
- [36] Solar radiation calculator n.d., Available at:

- <https://www.timeanddate.com/weather/uk/london/>, [accessed April 16, 2020].
- [37] Senwei energy n.d., Available at: <http://www.windpowercn.com/>, [accessed April 16, 2020].
- [38] M. Zare, R. Azizipanah-Abarghooee, R. Hooshmand, M. Malekpour, Optimal reconfiguration of distribution systems by considering switch and wind turbine placements to enhance reliability and efficiency, *IET Generation, Transmission Distribution* 12 (6) (2018) 1271–84.
- [39] M. Jadidbonab, B. Mohammadi-Ivatloo, M. Marzband, P. Siano, Short-term self-scheduling of virtual energy hub plant within thermal energy market, *IEEE Transactions on Industrial Electronics* (2020) 1–1.
- [40] R. Das, Y. Wang, G. Putrus, R. Kotter, M. Marzband, B. Herteleer, J. Warmerdam, Multi-objective techno-economic-environmental optimisation of electric vehicle for energy services, *Applied Energy* 257 (2020) 113965.
- [41] M. A. Mirzaei, A. Sadeghi-Yazdankhah, B. Mohammadi-Ivatloo, M. Marzband, M. Shafie-khah, J. ao P.S. Catalão, Integration of emerging resources in igdt-based robust scheduling of combined power and natural gas systems considering flexible ramping products, *Energy* 189 (2019) 116195.
- [42] M. Pourakbari-Kasmaei, M. Lehtonen, M. Fotuhi-Firuzabad, M. Marzband, J. R. S. Mantovani, Optimal power flow problem considering multiple-fuel options and disjoint operating zones: A solver-friendly MINLP model, *International Journal of Electrical Power Energy Systems* 113 (2019) 45–55.